In Silico Identification, Characterization and Diversity Analysis of RNAi Genes and their Associated Regulatory Elements in Sweet Orange (*Citrus sinensis L)*

Md. Parvez Mosharaf[1], Md. Asif Ahsan[1], Hafizur Rahman[3], Zobaer Akond[1,4,5], Fee Faysal Ahmed[1], Md. Mazharul Islam[1], Mohammad Ali Moni[2], Md. Nurul Haque Mollah[1]*

[1]Bioinformatics Laboratory, Department of Statistics, University of Rajshahi, Rajshahi-6205, Bangladesh, [2]The University of Sydney, Sydney Medical School, School of Medical Sciences, Discipline of Biomedical Science, Sydney, New South Wales, Australia, [3]Institute of Biological Sciences, University of Rajshahi, Rajshahi-6205, Bangladesh, [4]Institute of Environmental Science, University of Rajshahi, Rajshahi-6205, Bangladesh, [5]Agricultural Statistics and ICT Division, Bangladesh Agricultural Research Institute (BARI), Gazipur, Bangladesh.

Corresponding Author: *Md. Nurul Haque Mollah; Bioinformatics Laboratory, Department of Statistics, University of Rajshahi, Rajshahi-6205, Bangladesh Tel: +880-0721-711557; E-mail: mollah.stat.bio@ru.ac.bd

Abstract: RNA interference (RNAi) plays key roles in post-transcriptional and chromatin modification levels as well as regulates various eukaryotic gene expressions which involved in stress responses, development and maintenance of genome integrity during developmental stages. The whole mechanism of RNAi pathway is directly involved with the gene-silencing process by the interaction of Dicer-Like (DCL), Argonaute (AGO) and RNA-dependent RNA polymerase (RDR) gene families. However, the genes of these three RNAi families are largely unknown yet in sweet orange (*Citrus sinensis),* though it is an economically important fruit plant all over the world. Therefore, a comprehensive investigation for genome-wide identification, characterization and diversity analysis of RNA silencing genes in *C. sinensis* was conducted and identified 4 CsDCL, 8 CsAGO and 4 CsRDR as RNAi genes. To characterize and validate the predicted genes of RNAi families, various bioinformatics analysis was conducted. Phylogenetic analysis clustered the predicted CsDCLs, CsAGOs and CsRDRs genes into four, six and four subgroups with the relevant genes of Arabidopsis respectively. The domain and motif composition analysis, the gene structure for all three-gene families exhibited almost homogeneity within the same group members while showed significant differences in between groups. The GO enrichment analysis results clearly indicated that the predicted genes have direct involvement into the RNAi process as expected in *C. sinensis*. Moreover, *Cis*-regulatory elements and regulatory transcription factor analysis of the reported RNAi genes demonstrated the diverse connection to the huge biological functions and regulatory pathways. The expressed sequence tag (EST) analysis showed that these genes are highly expressed in fruit and leaves which indicate that these reported genes have great involvement in *C. sinensis* food, flowering and fruit production. The expression analysis of the reported RNAi genes might be more useful to explore the most effective RNAi genes in *C. sinensis* for further biotechnological application.

Keywords: RNAi genes, Transcription Factor, Cis-elements, Expressed Sequence Tag, Gene ontology, Bioinformatics approach, *C. sinensis*

1. INTRODUCTION

In multicellular eukaryotes, wide range of biological functions including genome rearrangement, antiviral defense, heterochromatin formation and development patterning and timing are fine-tuned by generally two types of small RNA (sRNA; including 21-24 nucleotides), named microRNA (miRNA) and short interfering RNA (siRNA) [1-3]. These sRNA molecules are initially involved with both transcriptional silencing and post-transcriptional RNA interfering RNA formation [2]. In plants, the sRNA biogenesis process is significantly regulated by the proteins encoded by respective Dicer-like (DCL), Argonate (AGO) and RNA-dependent RNA polymerases (RDR) gene families. The DCLs are deeply related to process the complementary dsRNAs into sRNAs especially 21-24 nucleotides longer (i.e. siRNA or miRNA). The specification to the endonuclease-containing, RNA-induced silencing complex (RISC) is provided by these sRNAs which facilitate the AGO proteins with RNaseH-type activities to degrade the target homologous RNAs with the sequence complementary to the small RNAs. These also refer to the transcriptional gene silencing by the implementation of chromatin reformation [4, 5].

A major component of RNA interference (RNAi) pathway (also known as small RNA (sRNA) biogenesis process), called DCL proteins which mainly process the small mature RNAs from the long double-stranded RNAs [6-10]. The important characteristic of these DCL proteins that having the functional domains, named DEAD/ResIII, Helicase_C, Dicer_Dimer, PAZ, RNase III and DSRM [11]. The PAZ domain acts to bind the siRNA as well as the dsRNA is cleaved by the two catalytic RNaseIII domains. The main components of RNAi are the AGO proteins which play the core roles of RNA silencing [12]. All the AGO proteins include the Argo-N/Argo-L, PAZ, MID and PIWI significant functional domains [13]. A significant specific binding pocket is contained in the PAZ domain. Additionally, to anchor the sRNA onto the AGO proteins, the specific pocket of MID domain binds the 5′ phosphate of the small RNAs [14]. The siRNA5′ end is bonded to the target RNA by the PIWI domain [15]. Among the three groups of AGO proteins i.e. Ago -like, PIWI-like and *C. elegens*-specific group 3 AGO proteins [16, 17], the Ago-like proteins are presented and expressed in plants, animals, fungi and bacteria, while PIWI-like proteins have only found in animals [18]. Some important catalytic residues are missed by *C. elegens*-specific group 3 AGO proteins [16] but others conserved as well as the expression of PIWI-like group is restricted in human germ-cell and in rat and some mammals [18]. The third major RNAi protein is RDR which have not been identified in insects or vertebrates [19] but present in fungi, nematodes and plants. These proteins are closely related to the various types of gene silencing [13].

In case of plants, multiple genes belong to the DCL, AGO and RDR gene families related to distinct RNAi pathways [20-22]. The member of these RNAi gene families has been identified in many plants species (such as Arabidopsis [23], rice [13], maize [24], tomato [25], tobacco [26], foxtail millet [27], and grapevine [28], cucumber [29], pepper [30]). In Arabidopsis, AtDCL1, AtDCL3 and AtAGO4 influenced the RNA-directed DNA methylation of the *FWA* transgene linkage to the histone H3 lysine 9 (H3K9) methylation [31, 32]. AtDCL2 is associated with the virus defence and siRNA production when the AtDCL4 is related to the regulation of vegetative phase change [11, 33]. AtDCL1 and AtDCL3 function for Arabidopsis flowering [34]. Moreover, in rice if the OsDCL1 is knocked down then it fails to perform siRNA metabolism which results pleiotropic phenotype in rice [35].

Besides, AGO proteins related to various forms of RNA silencing, such as AtAGO1 is associated with the transgene-silencing pathways [36] and AtAGO4 with the epigenetic silencing [31]. AtAGO7 and AtAGO10 influence the plant growth [37] and meristem maintenance [38]. Additionally, others AGOs also have a significant role in RNAi pathways. On the other hand, previous studies reported that the RDR genes are responsible for different gene silencing including co-suppression, virus defence, chromatin silencing and PTGS in plants such as in Arabidopsis, maize [21, 39-42].

However, the genes of these three RNAi families are largely unknown yet in the economically important fruit plant *C. sinensis*. The sweet orange (*C. sinensis*) is considered as an inevitable source of high nutrition, a great natural source of vitamin C, an unavoidable antioxidant important for the human body [43]). In production volume, orange is the world second fruit plant all over the world (FAO Statistics 2006). Not only having the market value, but also sweet orange contains about 170 phytonutrients and over 60 flavonoids those works as antioxidant, anti-inflammation, anti-cancer and anti-arteriosclerosis compound and also protects from many chronic diseases like arthritis, obesity and coronary heart diseases [44-47]. Therefore, a comprehensive investigation for genome-wide identification, characterization and diversity analysis of RNAi genes in *C. sinensis* is essential. In this project, an attempt is made to accomplish a comprehensive *in silico* investigation for genome-wide identification, characterization and diversity analysis of the members of DCL, AGO and RDR gene families in *C. sinensis*. A number of bioinformatics analysis such as, phylogenetic analysis, gene structure, functional domains and motifs, gene ontology (GO), sub-cellular localization, transcription factor (TF) analysis, cis-acting regulatory element and expressed sequence tag (EST) analysis have been considered to characterize and validate the predicted RNAi genes in *C. sinensis*.

2. MATERIALS AND METHODS

2.1. Identification of DCL, AGO and RDR Genes

For genome-wide identification of DCL, AGO and RDR genes in sweet orange (*C. sinensis*), protein sequences were downloaded from the Phytozome database (https://phytozome.jgi.doe.gov/pz/portal.html). In this purpose, the previously identified sRNA biogenesis protein sequences of the model plant *Arabidopsis thaliana* (AtDCLs, AtAGOs and AtRDRs) were used to search the protein sequence of *C. sinensis*. The Basic Local Alignment Search Tool (BLASTP) program was used against *C. sinensis* genome in the Phytozome database (Fig. **(1)**).

Fig. (1). The working flowchart to select the best candidates for DCL, AGO and RDR genes in *C. sinensis*.

The resulted paralogs protein sequences from *C. sinensis* were downloaded with the significant score (≥50) and the significant E-values. For avoiding the redundancy of sequences, only the primary transcripts were considered in this analysis. The conserved domains of all retrieved sequences were searched and predicted by using the Pfam (http://pfam.sanger.ac.uk/) and the NCBI-CD database (http://www.ncbi.nlm.nih.gov/Structure/cdd/wrpsb.cgi) and the SMART analysis. By this time, the different genomic information including the primary transcript name, genomic length, the chromosomal location of genes, encoded protein length were downloaded from the *C. sinensis* genome in Phytozome database. In this study, the computationally identified new CsDCLs, CsAGOs and CsRDRs genes in *C. sinensis* genome were named according to the nomenclature based on phylogenetic relatedness of the similar family-members of the *Arabidopsis thaliana* genes as named previously. The molecular weight of the selected protein sequences was predicted by using the ExPASyComputepI/Mwtool (http://au.expasy.org/tools/pito ol.html).

2.2. Sequence Alignment and Phylogenetic Analysis

In this *in silico* identification, the multiple sequence alignments of the encoded protein sequences of the predicted genes were conducted by using the Clustal-W method [48] with the MEGA5 program [49]. Finally, the phylogenetic tree analysis was carried out using the Neighbor-joining method [50] implemented on the aligned sequenced and the 1,000 bootstrap replicates [51] were used to check this evolutionary relationship. The evolutionary distances were computed using the Equal Input method [52].

2.3. Conserved Domain and Motif Analysis

To investigate the functional domains of the predicted genes by GENEDOC program using the aligned sequences although domains were predicted according to the NCBI database, Pfam database and SMART analysis (Fig. **(1)**). The CsDCLs, CsAGOs and CsRDRs proteins reflected multiple functional domains like the AtDCLs, AtAGOs and AtRDRs proteins. The predicted genes were selected containing the maximum number of functional domains similar to the AtDCLs, AtAGOs and AtRDRs. For DCL proteins, all six functional domains i.e. DEAD/ResIII, Helicase_C, Dicer_Dimer, PAZ, RNase III and DSRM were considered to choose the prominent CsDCL candidates in *C. sinensis.* Similarly, the proteins were sorted out as CsAGO candidate having the Argo-N/Argo-L, PAZ, MID and PIWI significant functional domains, the characteristic of plant AGO proteins. Same approach was applied to discriminate the CsRDRs genes. In motif investigation, the most significant conserved metal-chelating catalytic triad residues in the PIWI domain, i.e. aspartate, aspartate and histidine (DDH) [13] as well as histidine at 798 positions (H798) were considered for CsAGOs (Fig. **(2)**). In this study, we considered the alignment of CsAGOs with the paralogs AtAGOs using Clustal-W method as mentioned before. Furthermore, the conserved motif divergences among all the predicted genes were conducted by a complete online protein sequence analysis using Multiple Expectation Maximization for Motif Elicitation (MEME-Suite) [53]. For this purpose, the following parameters were specified: (i) optimum motif width as ≥6 and ≤50; (ii) maximum 20 motifs.

2.4. Gene Structure Analysis

For further computational analysis, we have considered the predicted gene structure and their interaction network analysis (Fig. **(1)**). The gene structure was analyzed using the online Gene Structure Display Server (GSDS 2.0, http://gsds.cbi.pku.edu.cn/index.php). The structures of the selected genes were compared with the gene structure of *Arabidopsis thaliana.* These combined gene structure Figures revealed the exon-intron composition of the predicted gene in *C. sinensis.* Moreover, numbers of intron were noted from GSDS.

2.5. Gene Ontology and Sub-cellular Localization Analysis

To check the engagement of our predicted RNAi associated genes with the cluster of different biological processes and molecular functional pathways, the GO analysis was conducted using online tool implemented in PlantTFDB[54]. Here, the respective p-values were determined by Fisher's exact test and Benjamini-Hochberg's technique was chosen for multiple testing corrections. We considered the p-value < 0.05 as statistical significant for the GO enrichment results corresponding to the predicted genes. For the reported gene product, the sub-cellular location was investigated into the cell considering the different organelles (Fig. **(1)**). these allocations could improve the overall understanding of the proposed genes as well as proteins functional pathways through the RNAi process. Web-based integrative subcellular location predictor tool called plant subcellular localization integrative predictor (PSI) [55] was used to predict the subcellular location of the identified genes.

2.6. Identification of Regulatory Relationship between TFs and *C. sinensis* RNAi genes

In every living organism, transcription levels of genes are directly regulated by the expression or suppression activities of transcription factors (TF) associated with the respective genes. TFs are also a kind of protein which can bind to the specific promoter region of the genes and can control the transcription process whether the genes to be expressed or suppressed. TFs are involved in the plant stress response activities; plant development in different life stage, disease resistance and so on. In this study, the analysis of associated TFs family with the predicted RNAi genes in *C. sinensis* was conducted from the widely used plant transcription factor database, plantTFDB (http://planttfdb.cbi.pku.edu.cn//). The related TFs were also categorized into 27 different TFs families and their roles in plants are also provided. These TFs are extremely important to study for the development of *C. sinensis* plant and enrich the sweet orange production.

2.7. Construction of Regulatory Network between TFs and *C. sinensis* RNAi genes

After identification of the related regulatory TFs of the *C. sinensis* RNAi genes, the regulatory network and sub-network were constructed and visualized using Cytoscape 3.7.1 [56] to find out the hub proteins and the related important TF through the interaction network. The networks were constructed to investigate the regulatory relationship between the TFs and RNAi genes.

2.8. *Cis*-regulatory element Analysis

In genetic transcription, the *cis*-elements are highly associated by controlling the transcription of a specific gene through the regulatory transcription factors. To collect more related genomic information about the *C. sinensis* RNAi genes, the CIs-acting regulatory element In the promoter region was retrieved and analyzed through the online c*is*-element prediction database PlantCARE (http://bioinformatics.psb.ugent.be/ webtools/plantcare/html/). The collected *cis*-regulatory element was categorized into five categories like light responsive (LR), stress responsive (SR), hormone responsive (HR), others activities (OT) and unknown function. The cis-element having known and described function are represented into the Fig. 12 for CsDCLs, CsAGOs and CsRDR separately.

2.9. *In silico* Expressed Sequence Tag (EST) Analysis

For the important and valuable information about the gene expression, the *in silico* expressed sequence tag (EST) data analysis was conducted. The PlantGDB (http://www.plantgdb.org/cgi-bin/blast/PlantGDB/) was used for EST mining against the proposed RNAi genes in *C. sinensis*. The default parameter with e-value=1e-10 were considered for blastn search for the EST mining in PlantGDB database. The further heatmap was constructed to represent the specific RNAi gene expression into different tissue and organ in this fruit plant.

3. RESULTS AND DISCUSSION

3.1. Identification and characterization of CsDCLs, CsAGOs and CsRDRs genes

To identify the best candidates of RNAi pathway in *C. sinensis* similar to the *A. thaliana,* all the previously downloaded sequences were gone throughout various kinds of analysis (Fig. **(1)**). Finally, we have isolated 4 DCL genes, 8 AGO genes and 4 RDR genes those produce the CsDCLs proteins, CsAGOs and CsRDRs proteins respectfully in the *C. sinensis* genome. On the basis of HMMER analysis with regards of all six types of conserved domains DEAD, Helicase_C, Dicer_dimar, PAZ, RNase III and DSRM; four DCL loci were identified in sweet orange genome. From the conserved domain search by Pfam databases, NCBI databases and the SMART analysis, all reflected that half of the predicted proteins (CsDCL1 and CsDCL4) are conserved with the DEAD/ResIII, Helicase_C, Dicer-dimer, PAZ, RNase III and dsRM domains, which are preserved by all the plant DCL proteins from the DCL genes family (class 3 RNase III family) [57, 58]. On the other hand, CsDCL2 and CsDCL3 have missed a single DSRM domain while others are contained with a second DSRM domain. This DsRM domain is lacked in by non-plant DCL completely [11]. Compared to others DCL proteins, the CsDCL1 has the N-terminal DEAD domain which might consist of three adjacent segments of amino acid sequence within the full domain length (152 amino acids), resulted by the analysis of Pfam databases and SMART. The CsDCL3 also revealed the ResIII domain instead of the

DEAD domain. Additionally, the genome length of predicted CsDCL genes varied from 10603 bp to 12728 bp corresponding to CsDCL1 and CsDCL2 with the coding potentiality of 1931 and 1396 amino acid (Table **(1))**.

Based on the conserved domain PAZ and PIWI from the putative polypeptide sequences by HMM and HMMER analysis, we have isolated a total of 8 AGO genes in the *C. sinensis* genome. Conserved domain analysis by the Pfam database, NCBI databases and SMART analysis, reported that all the selected AGO proteins (CsAGO1-8) shared an N-terminus PAZ domain and a C-terminus PIWI super family domain, the core properties of plant AGO proteins. Moreover, the CsAGO proteins also preserved the other domains like the Arabidopsis i.e. ArgoN, ArgoL1, DUF1785, ArgoL2, ArgoMid.

Table 1: Basic information about *C. sinensis* Dicer-like, Argonaute and RNA-dependent RNA polymerase gene families.

Serial Number	Gene Name	Accession Number	Chromosomal location	Gene Length (bp)	Protein				Type
					No. of Intron	Molecular Weight (D.a)	Protein Length (a.a)	PI	
CsDCLs									
1	CsDCL1	orange1.1g000174m	scaffold00001:3480331..3490933	10603	18	216424.20	1931	5.96	DCL 1
2	CsDCL2	orange1.1g000607m	scaffold00367:74912..87639	12728	21	158487.91	1396	7.65	DCL 2
3	CsDCL3	orange1.1g000379m	scaffold00013:998934..1009643	10710	24	178949.30	1604	8.01	DCL 3
4	CsDCL4	orange1.1g000380m	scaffold00068:219006..230745	11740	25	179592.47	1601	6.46	DCL 4
CsAGOs									
1	CsAGO1	orange1.1g001466m	scaffold00674:51962..59926	7965	20	118338.09	1073	9.38	AGO 1
2	CsAGO4	orange1.1g002449m	scaffold00028:907375..916121	8747	21	102997.53	920	8.98	AGO 4
3	CsAGO5a	orange1.1g002204m	scaffold00595:85931..92382	6452	21	106772.65	954	9.27	AGO 5
4	CsAGO5b	orange1.1g037086m	scaffold00595:96826..99593	2768	10	48003.28	426	9.05	AGO 5
5	CsAGO5c	orange1.1g003630m	scaffold03700:12..6517	6506	21	91163.31	806	9.03	AGO 5
6	CsAGO6	orange1.1g002661m	scaffold00067:338566..346634	8069	21	100499.54	895	9.41	AGO 6
7	CsAGO7	orange1.1g001684m	scaffold00003:3309646..3313553	3908	2	117035.78	1030	9.24	AGO 7
8	CsAGO10	orange1.1g001954m	scaffold00011:54251..63917	9667	20	111515.83	992	9.34	AGO 10
CsRDRs									
1	CsRDR1	orange1.1g002586m	scaffold00058:231382..236081	4700	2	103382.03	904	6.51	RDR 1
2	CsRDR2	orange1.1g001183m	scaffold00020:1255446..1250927	4520	3	128958.15	1131	6.59	RDR 2
3	CsRDR3	orange1.1g001771m	scaffold00027:638984..650509	11526	18	115670.83	1015	6.80	RDR 3
4	CsRDR6	orange1.1g041430m	Scaffold d00051:398116..402488	4373	1	136437.20	1157	6.13	RDR 6

[Information containing the gene names, accession number, chromosomal location, genome length, protein length were collected from Phytozome database (https://phytozome.jgi.doe.gov/pz/portal.html) and the molecular weight and PI values were predicted by the ExPASy ComputepI/Mwtool (http://au.expasy.org/tools /pi_tool.html). Molecular weights are in Daltons and "aa" means amino acid.]

From the previous study, the PIWI domain demonstrating expansive homology to RNase H binds the siRNA 5′ end to the target RNA [15] and cracks the target RNAs that represents the complementary sequences to small RNAs [59]. Interestingly, the catalytic traid, three conserved metal-chelating residues (D=aspartate, D=aspartate and H=histidine) in PIWI domain are related to the previous event and this traid was firstly showed in the model plant Arabidopsis on AGO1 [13].

Moreover, another critical conserved histidine residue in AGO1 for *in vitro* endonuclease activity [60] was found. The genome length of the selected CsAGO genes varied from 2768 bp to 9667 bp producing the CsAGO5b and CsAGO10 respectively with the coding potentiality of 426 and 992 amino acids. In this study, the multiple sequence alignment of the PIWI domains of all CsAGOs with the paralogs AtAGOs in Arabidopsis using the CLUSTAL-W method (Fig. **(2)**).

Fig. (2). The multiple sequence alignment profile of PIWI domain of the amino acids sequences of *C. sinensis* and Arabidopsis AGO proteins by Clustal-W program in MEGA5. The downward yellow arrows indicate the position of conserved DDH traid of PIWI domain and the conserved H798 positions are surrounded by red box.

This alignment revealed that the five CsAGOs represented the conserved DDH traid residues like Arabidopsis AGO1. Among the other three CsAGOs, the CsAGO5b represented two missing PIWI domain catalytic residue(s) in the second aspartate at the 845th position (D845) and third histidine at the 986th position (H986) (Table **(2)**). But the other two CsAGO proteins, CsAGO5a and CsAGO5c has the catalytic traid but with a replacement in the third histidine residue at the 986th position by tyrosine (Y) residue.

Table 2: Comparison of the argonaute proteins with missing catalytic residue(s) in PIWI domains between *C. sinensis* and *A. thaliana.*

Serial No.	*Citrus sinensis*		*Arabidopsis thaliana*[b]	
	Argonaute	Motifs[a]	Argonaute	Motifs[a]
1	CsAGO1	DDH/H	AtAGO1	DDH/H
2	CsAGO4	DDH/P	AtAGO4	DDH/S
3	CsAGO5a	DDY/H	AtAGO5	DDH/H
4	CsAGO5b	D_ _ /R	AtAGO6	DDH/P
5	CsAGO5c	DDY/P	AtAGO7	DDH/H
6	CsAGO6	DDH/S	AtAGO10	DDH/H
7	CsAGO7	DDH/H		
8	CsAGO10	DDH/H		

[a] Comparison of conserved motif corresponds to D760, D845, H986/H798 of Arabidopsis AGO1; D: aspartate, H: histidine, P: proline, R: arginine, S: serine, Y: tyrosine and "_" represents the missing catalytic residue(s).

[b] From Kapoor et al. (2008)

Surprisingly, the histidine residue at the 786th position was replaced by proline (P) in CsAGO4 and CsAGO5c; by arginine (R) in CsAGO5b and in CsAGO6, H786 residue was replaced by serine (S) residue (Table **(2)).** The newly identified 4 CsRDRs proteins that shared a common domain RdRP which consist of a sequence motif corresponds to the catalytic β' subunit of DNA-dependent RNA polymerases [61]. The CsRDRs have the genome length varied from 4373 bp to 11526 bp corresponding coding potentiality of 1157 and 1015 amino acids for CsRDR6 and CSRDR3 respectively.

3.2. Phylogenetic Analysis of DCL, AGO and RDR proteins in *C. sinensis* and *A. thaliana*

In order to conduct the phylogenetic relationship analysis among the DCL, AGO and RDR proteins of sweet orange and Arabidopsis, the total length amino acid sequences of these plants were used to assess the evolutionary history throughout the neighbor-joining phylogenetic tree (Fig. **(3)**)construction method with considering 1000 bootstrap values. Phylogenetic tree was generated from the full-length aligned protein sequences (**S**upplementary Data **S1**) of the 4 CsDCLs and 4 AtDCLs from *C. sinensis* and Arabidopsis (Fig. **(3A)**).The tree represented four subfamilies of newly identified CsDCL proteins i.e. CsDCL1, CsDCL2, CsDCL3 and CsDCL4 corresponding to the DCLs in Arabidopsis on the basis of high similarity of AtDCL1, AtDCL2, AtDCL3 and AtDCL4 respectively with well-supported bootstrap values. The CsDCL proteins showed high sequence conservation with their corresponding counterpart in Arabidopsis. Every DCL subfamily comprised a single CsDCL protein.

To construct the phylogenetic tree for CsAGO proteins, the full-length multiple aligned protein sequence of the 8 CsAGOs and 6 AtAGOs were considered (Supplementary Data **S2**). The tree exhibited six subfamilies, AGO1, AGO4, AGO5, AGO6, AGO7 and AGO10 with the higher sequence similarity (Fig. **(3B)**). The AGO1 subfamily consists only a single Citrus protein named CsAGO1 with the Arabidopsis AGO protein AtAGO1. Among the other AGO subfamilies, each showed a group containing a single Citrus AGO protein with a single Arabidopsis AGO protein, except AGO5 cluster.

Fig. (3). Phylogenetic tree for the (A) Dicer-like (DCL) proteins (B) Argonaute (AGO) proteins and (C) RDR proteins from Citrus and Arabidopsis. All the phylogenetic trees were constructed by neighbour-joining method considering significant bootstrap values. The accession number and the abbreviations of proteins from Arabidopsis are given below while others are tabulated in (Table 1): (A) Four DCL proteins, AtDCL1 (At1g01040), AtDCL2 (At3g03300), AtDCL3 (At3g43920) and AtDCL4 (At5g20320) were used in DCL analysis. (B) AtAGO1 (At1g48410), AtAGO4 (At2g27040), AtAGO5 (At2g27880), AtAGO6 (At2g32940), AtAGO7 (At1g69440) and AtAGO10 (At5g43810) were considered for AGO analysis. (C) Among six AtRDR proteins, the phylogenetic tree exhibited only four major classes with CsRDR proteins. The RDR proteins from Arabidopsis were AtRDR1 (At1g14790), AtRDR2 (At4g11130), AtRDR3 (At2g19910) and AtRDR6 (At3g49500). The three different gene families from Arabidopsis are indicated by coloured in the constructed tree adjacent to the designation.

The AGO5 subfamily included three citrus proteins with a single Arabidopsis protein AtAGO5, which were named CsAGO5a, CsAGO5b and CsAGO5c on the basis of higher sequence similarity to AtAGO5. The AGO1, AGO4, AGO6, AGO7 and AGO10; these groups exhibited each separated cluster with a single AGO protein from Citrus and a single protein from Arabidopsis. The clustered citrus AGO proteins were designated as CsAGO1, CsAGO4, CsAGO6, CsAGO7 and CsAGO10 respectively based on high sequence similarity to their corresponding pair AGO protein from Arabidopsis.

Four main classes of RDR genes in Citrus were revealed by the phylogenetic analysis of the full length aligned polypeptide sequences (Supplementary Data **S3**) of RDR proteins of Citrus and Arabidopsis shown in (Fig. **(3C)**). The CsRDR proteins were designated as CsRDR1, CsRDR2, CsRDR3 and CsRDR6 corresponding to the RDR proteins of Arabidopsis AtRDR1, AtRDR2, AtRDR3 and AtRDR6 respectively for the increased sequence similarity. The predicted CsRDR proteins were clustered according to their high sequence conservation with their reflection part in Arabidopsis RDR proteins.

3.3. Conserved Domain and motifs analysis of predicted proteins

Preliminary domain analysis of the predicted CsDCLs, CsAGOs and CsRDRs were conducted for searching the conserved domains by Pfam databases, NCBI-CDD databases and Simple Modular Architecture Research Tool (SMART) analysis, results are tabulated in (Table **(3)**).

Table 3: Domain analysis of the DCLs, AGOs and RDRs proteins of the predicted gene mapping on *C. sinensis* with Pfam, SMART and NCBI-CDD.

Serial Number	Gene Name	Accession Number	Domains		
			Pfam	SMART	NCBI-CDD
CsDCLs					
1	CsDCL1	orange1.1g000174m	DEAD, Helicase_C, Dicer_dimer,PAZ, Ribonuclease_3,Ribonuclease_3, dsrm, DND1_DSRM	DEXDc, Helicase_C, Dicer_dimer, PAZ, RIBOc, RIBOc, DSRM, DSRM	PAZ super family, helicase_C, Rnc, RIBOc, Dicer_dimer, DSRM
2	CsDCL2	orange1.1g000607m	DEAD, Helicase_C, Dicer_dimer, PAZ, Ribonuclease_3, Ribonuclease_3	DEXDc, Helicase_C, Dicer_dimer, PAZ, RIBOc, RIBOc	helicase_C, RIBOc , PAZ super family, Dicer_dimer, RIBOc
3	CsDCL3	orange1.1g000379m	ResIII,Helicase_C, Dicer_dimer, PAZ, Ribonuclease_3	DEXDc, Helicase_C, Dicer_dimer, Low complexity PAZ, RIBOc	helicase_C, PAZ super family ,RIBOc, Dicer_dimer, Rnc super family
4	CsDCL4	orange1.1g000380m	DEAD, Helicase_C, Dicer_dimer, PAZ, Ribonuclease_3, Ribonuclease_3, DND1_DSRM	DEXDc, Helicase_C, Dicer_dimer, PAZ, RIBOc, RIBOc, DSRM, DSRM	helicase_C, RIBOc, Dicer_dimer, RIBOc, PAZ super family, DSRM
CsAGOs					
1	CsAGO1	orange1.1g001466m	Gly-rich_Ago1, ArgoN, ArgoL1, PAZ, ArgoL2, ArgoMid, Piwi	Gly-rich_Ago1, ArgoN, DUF1785, ArgoL1, PAZ, ArgoL2, ArgoMid, Piwi	Piwi-like super family, Gly-rich_Ago1
2	CsAGO4	orange1.1g002449m	ArgoN, ArgoL1, PAZ, ArgoL2, ArgoMid, Piwi	ArgoN, DUF1785, PAZ, ArgoL2, ArgoMid, Piwi	Piwi-like super family
3	CsAGO5a	orange1.1g002204m	ArgoN, ArgoL1, PAZ, ArgoL2, ArgoMid, Piwi	ArgoN, DUF1785, PAZ, ArgoL2, ArgoMid, Piwi	Piwi-like super family
4	CsAGO5b	orange1.1g037086m	PAZ, ArgoL2, ArgoMid, Piwi	PAZ, ArgoL2, ArgoMid, Piwi	Piwi-like super family, PAZ

5	CsAGO5c	orange1.1g003630m	ArgoN, ArgoL1, PAZ, ArgoL2, ArgoMid, Piwi	ArgoN, DUF1785, PAZ, ArgoMid, Piwi	Piwi-like super family
6	CsAGO6	orange1.1g002661m	ArgoN, ArgoL1, PAZ, ArgoL2, Piwi	ArgoN, DUF1785, PAZ, ArgoL2, Piwi	Piwi-like super family
7	CsAGO7	orange1.1g001684m	ArgoN, ArgoL1, PAZ, Piwi	ArgoN, DUF1785, PAZ, ArgoMid, Piwi	Piwi_ago-like, PAZ, ArgoL1, ArgoN
8	CsAGO10	orange1.1g001954m	ArgoN, ArgoL1, PAZ, ArgoL2, ArgoMid, Piwi	ArgoN, DUF1785, PAZ, ArgoL2, ArgoMid, Piwi	Piwi-like super family
CsRDRs					
1	CsRDR1	orange1.1g002586m	RdRP	RdRP	RdRP
2	CsRDR2	orange1.1g001183m	RdRP	RdRP	RdRP, RRM_SF super family
3	CsRDR3	orange1.1g001771m	RdRP	RdRP	RdRP
4	CsRDR6	orange1.1g041430m	RdRP	RdRP	RdRP

The CsDCLs proteins showed all the conserved domains through the SMART analysis exhibited some unknown regions and low complexity regions besides the expected domains (Fig. **(4)**). The conserved motifs were screened using MEME with the pre-discussed criterions. The CsDCLs, CsAGOs and CsRDRs proteins were performed all characteristic of DCL, AGO and RDR domain organization was found in Arabidopsis DCLs, AGOs and RDRs proteins respectively when the CsDCL3 has the ResIII domain instead of DEAD domain and CsAGO5b has missed the ArgoN domain having the PAZ and PIWI domain (Fig. **(4)**).

Fig. (4). The conserved domains of the predicted proteins were drawn by using Pfam database.

By MEME-suite analysis, the DCLs proteins have 19 (in CsDCL2 and CsDCL3) and 20 (in CsDCL1 and CsDCL4) motifs among the 20 motifs as mentioned before. The predicted motifs are well distributed among the DCL domains for all CsDCLs proteins The MEME analysis of CsAGOs proteins identified 16 common conserved motifs from 20 motifs among all the AGO proteins in *C. sinensis* and Arabidopsis, except the CsAGO5b having 9 conserved motifs. The predicted conserved motifs were distributed among the AGO domains in *C. sinensis* AGO proteins.

Among the CsAGO proteins one has 16 different motifs (CsAGO7), three proteins (CsAGO4, CsAGO5c and CsAGO6) reflected 17 motifs and others three proteins (CsAGO1, CsAGO5a and CsAGO10) contained 20 conserved motifs (Fig. **(5)**). Although from the analysis, it is observed that the well conservation within the AGO proteins of *C. sinensis* and Arabidopsis, there still has had some variability of motif distribution between the different subfamilies of AGO proteins in *C. sinensis.* Moreover, this analysis suggested that the conserved predicted motifs might play some vital functional roles in these AGO proteins.

Fig. (5). Conserved motifs of the proteins of different genes families are drawn by MEME-suite (maximum 20 motifs are displayed). Different color represented various motifs distributed in the domains of the proteins.

In RDR protein family, the MEME analysis exhibited that the least 6 conserved motifs in CsRDR3 coincided with the AtRDR3. Among other CsRDRs proteins, the CsRDR2 and CsRDR6 lighted 20 out of 20 conserved motifs which are well distributed on the RdRP domain and the CsRDR1 had 18 out of 20 conserved motifs (Fig. **(5)**). Although the predicted motifs were well conserved in the major part of the RDR domain, the motif schemes of different RDR subfamilies did not follow the same distributional pattern. The RDR proteins also reflected some additional motifs besides the RdRP domain having the unknown functional role. However, the MEME-suite analysis reflexed that the CsDCLs, CsAGOs and CsRDRs proteins are enriched with well conservation and distribution of the motifs throughout the subfamilies. This analysis suggested that the predicted motifs might play a different vital role in the functional importance of these genes in *C. sinensis* in different life stages.

3.4. Gene Structure and Genomic location of CsDCLs, CsAGOs and CsRDRs

To observe the gene structure of the predicted CsDCLs, CsAGOs and CsRDRs gene, their exon-intron configuration was explored by using GSDS with the respective genes family of Arabidopsis. The exon-intron configuration of the predicted genes represented higher conservation as expected for that of DCLs, AGOs and RDRs genes in the model plant Arabidopsis (Fig. **(6)**). The gene structure of CsDCLs exhibited having the number of intron 18-25 **(**Table **(1))**, correspondence according to higher similarity with AtDCLs.

Fig. (6). Gene structure of the predicted CsDCLs, CsAGOs and CsRDRs proteins in *C. sinensis* with Arabidopsis using Gene Structure Display Server (GSDS 2.0, http://gsds.cbi.pku.edu.cn/index.php) (Bo Hu et al. 2015).

On the other hand, out of eight CsAGOs, six genes displayed 20 or 21 introns in the gene structure except the CsAGO5b and CsAGO7 having the number of introns 10 and 2 respectively (Fig. **(6)**). This structure indicated that CsAGOs genes are highly similar to the AtAGOs. The CsRDRs showed up with the equal number of introns with their paralogs from Arabidopsis, except the CsRDR3 having a number of intron 18 which is just one short than introns in AtRDR3.

The genomic location of the predicted RNAi pathway related genes in *C. sinensis* was conducted by observing the position of the genes in different scaffold location. The predicted CsDCLs, CsAGOs and CsRDRs genes were distributed among the 15 different scaffolds through the entire genome (Supplementary Table **S1**). All proteins have a unique scaffold position while the two CsAGO genes (CsAGO5a and CsAGO5b) were placed in the scafold000595 in the different location. Most of the genes are situated from scafold00001 to scafold00674 where the CsAGO5c is in the scafold03700.

3.5. Gene Ontology Enrichment Analyses

In order to better understand the biological roles of the predicted RNAi genes and characterize them, GO enrichment analysis was performed (Fig. **(7)**, Supplementary Data **S4**). From the analysis result it was observed that 12 genes involved in post-transcriptional gene silencing (PTGS) pathway (GO:0016441; p-value:3.60e-27), 10 related to RNA interference (GO:0016246; p-value: 8.50e-25) and 12 genes are associated with gene silencing (GO:0016458; p-value:7.40e-24). The RNAi is closely related to the phenomenon named post-transcriptional gene silencing (PTGS) in plants [62].

Fig. (7). The heatmap for the predicted GO terms corresponding to the RNAi genes are presented for (A) biological process (B) cellular components (C) molecular function whether the genes are related (Present) or not (Absent). The p-value corresponds to the GO terms are showed in histogram adjacent to the heatmap, using -log10 (p-value). The Ven diagrams are drawn to observe the shared GO terms by three gene families considering the (D) biological process (E) cellular components (F) molecular functions.

The GO enrichment analysis showed that five predicted RNAi genes (among 16) are related to the endonuclease activity (GO: 0004519; p-value= 4.20e-09) which (Supplementary Data S4) indicates a positive linkage with the RNA-induced silencing complex (RISC-mediated) mediated cleavage activities into the cell. This multimeric protein complex (i.e. RISC) guides for protein degradation. Among the RNAi proteins, Argonautes work for the cleavage called endonucleolytic activities, which result the final PTGS for specific mRNA substrate [63]. By the GO analysis, there are 13 genes related to nucleic acid binding (GO: 0003676; p-value=1.10e-08), 7 genes to RNA binding (GO: 0003723; p-value=2.10e-07) and 12 genes related to protein binding (GO: 0005515; p-value= 0.00022) activities (Supplementary Data S4) which indicate the RNAi protein's participation to the RISC as well as interference processes. The predicted CsAGO proteins contain the special domains called PAZ and PIWI domain that play the key role in making a complex with RNA or DNA. The PAZ domain has a nucleic acid-binding fold that promotes the domain to bind to the specific position of the nucleic acids [64, 65]. The GO enrichment analysis also showed the attachment of the predicted genes to the numerous biological processes. Significantly, most of the reported genes are engaged with the regulation of biological process (GO:0050789; p-value=3.90e-08), negative regulation of gene expression (GO:0010629; p-value:2.30e-20) and dsRNA fragmentation (GO:0031050; p-value:4.10e-23) (Supplementary Data **S4**).

The *C. sinensis* RNAi genes are also involved in virus response (GO:0009615; p-value:6.70e-28), immune response (GO:0006955; p-value:4.10e-14) as these were reported for AtDCL and AtRDR[11, 21, 33, 39-42]. These GO enrichment analysis for biological processes (Supplementary Fig. **S1A**), molecular functions (Supplementary Fig. **S1B**) and cellular component (Supplementary Fig. **S1C**) undoubtedly indicated that the predicted genes are deeply interrelated with the RNAi pathway in *C. sinensis.* In addition, the predicted genes act with the hydrolase activity, acting on ester bond, predicted from the GO analysis (Supplementary Data **S4**).

The Ven Diagram of the GO terms for three clusters of the RNAi genes was drawn (Fig. **(7)**). It was observed that the CsDCL, CsAGO and CsRDR genes shared significant number of GO pathways in common. In biological process, there are 89 GO enrichment pathways (Fig. **(7)**) were shared by the reported proteins, which indicate the involvement of the RNAi gene members in numerous biological processes together. Also in molecular function and cellular component, the predicted genes exhibited a group of mutual GO pathways. So this GO analysis provides a significant indication of the predicted RNAi genes in this study.

3.6. Sub-cellular Localization of the Reported Genes and Proteins

The subcellular localization studies of the predicted proteins were observed to uncover their cellular appearance. By the sub-cellular localization annotation, it has been shown that all the reported proteins identified in this study appear into the cytosol (Fig. **(8)**). As PTGS occurs into the cytoplasmic region [66], this result implies that the reported RNAi proteins may directly involve to the PTGS process. On the other hand, four CsAGO and one CsRDR proteins exhibited their appearance into the nucleus when as no CsDCLs are located there. These bring a significant importance whether the CsDCLs are not found in nucleus. Further expression pattern analysis will provide deeper information about the CsDCLs. Some of the identified RNAi proteins are also distributed into the cell membrane, plastid and mitochondria (Fig. **(8)**).

Fig. (8). Sub-cellular localization analysis for (A) CsDCL (B) CsRDR and (C) CsAGO proteins. (D) The percentage of protein appears in different cellular components. Here cytosol (cytos), endoplasmic reticulum (ER), extracellular (extra), golgi apparatus (golgi), membrane (membr), mitochondria (mito), nuclear (nucl), peroxisome (pero), plastid (plast) and vacuole (vacu). Over all report is tabulated in (Supplementary Table **S2**).

Previous studies reported that the RNAi genes are not only highly related with PTGS but also with transcriptional gene silencing (TGS) [66]. In protein transcriptional process, RNA polymerase type II complexes are directly involved [67]. For PTGS, the RNAi proteins have greater participation in RNA-induced silencing complex (RISC-mediated) mediated cleavage activities by the help of DCL, AGO and RDR proteins with other molecules [63]. The PTGS happens into the cytoplasmic region for targeted mRNA protein degradation [67].

3.7. Regulatory Relationship between TFs and RNAi genes

TFs are considered as the switch of gene expression in all living organism. Plant TFs play significant role in growth, development and stress response activities [68]. Thus, identifying TFs regulating RNAi genes could help to improve our understanding of gene silencing process in *C. sinensis*. In this analysis a total of 235 TFs were identified those regulate the predicted RNAi genes (Supplementary Data **S5**). The identified TFs were distributed into 27 groups based on the TF families. The TFs MYB, Dof, ERF, NAC, MIKC_MADS, WRKY and bZIP families might play significant role in regulating RNAi genes. Particularly those of ERF, NAC, WRKY and bZIP families, which are the top four families those contained 29, 20, 20 and 10 TFs and accounted 57.66% of the total identified TFs (Supplementary Table **S3**). This finding indicated that those TFs could be important in regulating RNAi genes.

Fig. (9). (A) The regulatory network among the TFs and the predicted RNAi genes. The nodes of the network were colored based on RNAi genes and TFs. DCL, AGO and RDR genes were represented by blue, red and green node color respectively and the TFs were represented by yellow node color. Different node symbols were used for different families of TFs. Magenta node level were used for the hub TFs. **(B)**The map representing the associated number of TFs with the CsRNAi genes.

To better understand the regulatory relationship between TFs and RNAi genes, a regulatory network was constructed (Fig. **(9A)**). From the resultant network it is observed that different groups of TFs exhibited distinct structure. For example, TF belongs to ERF family mainly bind to the gene CsAGO5a (Fig. **(9B)**, Supplementary Fig. **S2**). However some RNAi genes such as CsAGO5c, CsDCL4 and others are regulated by ERF family; all of them are also linked to CsAGO5a (Fig. **(10A)**). Very similar results were also observed for the hub TFs NAC, WRKY and bZIP (Fig. **(10B-D)**).

Fig. (10). RNAi gene mediated sub-network for (A) ERF, (B) NAC, (C) bZIP, and (D) WRKY TF family. (E) Sub-network among the hub TFs those regulate more than five RNAi genes.

Moreover, six hub TFs were identified on the basis of node degree which have more than five interacting partners with the RNAi genes. Among them 3 belongs to dof family and other three are in MIKC_MSDS, C2H2 and bZIP (Fig. **(10E)**). The Dof TFs family is directly involved with the DNA binding activities by the N- and C-terminal region and causes the regulation of gene activation or repression of the target genes which is the main theme of RNAi. The Dof TFs family also works for the biosynthesis of flavonoids and glucosinolates, stress tolerance, seed germination and controlling the photoperiodic flowering [69-72]. The TF orange1.1g027691m (MIKC_MADS) regulates heights seven RNAi genes and the rest regulate five RNAi genes in the network (Fig. **(10E)**). The regulatory network clearly exposes that these predicted genes of RNAi process in *C. sinensis* will exhibit a dramatically expression pattern that can be retrieved by deeper investigation of these genes in future.

Besides, all of the hubs TFs are connected to eight RNAi genes. Of RNAi genes corresponding to hub TFs, five are AGO two are DCL and only one is RDR. Three RNAi genes (2 AGO: CsAGO10, CsAGO7; 1 DCL: CsDCL1) were predicted to be regulated by the entire six hub TFs.

Cis-acting regulatory element Analysis

The *cis*-acting regulatory element analyses were conducted to find out the functional diversity of the motifs related to the promoter region of the proposed RNAi genes into *C. sinenesis.* The PlantCARE database provided the information about the motifs and their functionality with the genes. The analysis revealed that most of the motifs were light responsive (LR) (Fig.

12), widely presents in the entire RNAi gene's promoter. Supporting the EST analysis, the light responsiveness is associated with the photosynthesis which occurs in leaf. Among the light responsive motifs the ATCT-motif, ATC-motif, Box-4, AE-box, G-box, I-box, GAT-motif, GT1-motif were shared by the most of the RNAi genes in *C. sinensis* (Fig. 12). The TC-rich repeats (cis-acting element involved in defense and stress responsiveness), MBS (MYB binding site involved in drought-inducibility) and LTR elements (*cis*-acting element involved in low-temperature responsiveness) were commonly found as stress responsive motif among the CsDCL/AOG/RDR genes in *C. sinensis*. It is known that the plant hormones are essential for plant growth and development.

Fig. (12). The *cis*-regulatory element in the promoter region of the identified *C. sinenis* DCLs, AGOs and RDRs genes respectively. The deep color represents the presence of that element with the corresponding genes.

The significant plant hormone responsive (HR) *cis*-acting element were identified in this analysis. The ABRE (cis-acting element involved in the abscisic acid responsiveness), AuxRR-core (cis-acting regulatory element involved in auxin responsiveness), GC-motif (enhancer-like element involved in anoxic specific inducibility), GARE-motif (gibberellin-responsive element), O2-site (cis-acting regulatory element involved in zein metabolism regulation), P-box (gibberellin-responsive element), TATC-box (cis-acting element involved in gibberellin-responsiveness), TCA-element (cis-acting element involved in salicylic acid responsiveness) and TGA-element (auxin-responsive element) were the hormone responsive *cis*-element shared by the CsDCLs, CsAGOs and CsRDRs as phytohormones responsiveness element (Fig. 12). There are some others significant elements were identified and represented as others activities. The AT-rich element (binding site of AT-rich DNA binding protein (ATBP-1)), AT-rich sequence (element for maximal elicitor-mediated activation), CAAT-box (common cis-acting element in promoter and enhancer regions), CAT-box (cis-acting regulatory element related to meristem expression), CCAAT-box (MYBHv1 binding site), GCN4_motif (cis-regulatory element involved in endosperm expression), TATA-box (core promoter element around -30 of transcription start), circadian (cis-acting regulatory element involved in circadian control), silencer (GT-1 factor binding site) and TGACG-motif (cis-acting regulatory element involved in the MeJA-responsiveness) were recognized as others cis-acting regulatory element shared by RNAi genes in *C. sinensis* (Fig 12). Some unknown cis-regulatory elements were also detected along with the reported cis-elements (Supplementary Table S6). In general the cis-regulatory elements carried out significant evidences about the proposed RNAi genes that will be helpful for further investigation about their role in plant disease response, growth and development.

In silico Expressed Sequence Tag (EST) Analysis

For the important and valuable information about the gene expression, the expressed sequence tag (EST) data analysis can bring a significant piece. This analysis helps to validate the genes activities and to investigate the activities in various stress conditions. The EST mining results from the PlantGDB database indicated that the RNAi genes of *C. sinensis* expressed in multiple important tissue and organs. However, the expression evidence of the RNAi genes in several species has been reported which showed that the RNAi genes have expression in leaf, root, flower, seeds and in others tissue [13, 23-30, 73]. The *in silico* expressed sequence tag (EST) analysis of the proposed *C. sinensis* RNAi genes showed that all the genes have their expression at least in one organ or tissue. In general, most of the genes were expressed in leaf and fruit which indicate that these genes have a direct involvement with the photosynthesis and fruit developmental stages in *C. sinensis* (Fig. 11).

Fig. (11). The *in silico* expressed sequence tag (EST) analysis of the identified RNAi genes in C. sinensis plant. The green color represents the existence of expression and off color stands for absent of expression.

The expression of CsDCLs were identified in leafs (CsDCL1/3/4), flowers (CsDCL2/4), fruit (CsDCL1/2/4), ovule (CsDCL1/3/4) and bark (CsDCL3), where no expression was found in root. The entire CsAGOs exhibited diverse expression pattern all over the plant through root, leafs, flowers, ovule, fruit, fruit rind and seed. Among the CsAGO genes, CsAGO1 and CsAGO4 were detected in maximum organs in *C. sinensis.* The only CsAGO1/4 provided the expression evidence into the seeds. Similarly the others RNAi genes, the CsRDRs also highly expressed into the leaf, flower and fruit when the CsRDR6 showed expression in ovule and bark. Interestingly, no expression evidence was found for the CsRDR3 in this *in silico* EST analysis (Fig. 11). According to the EST analysis, the proposed RNAi genes have vast contribution in ovule fertilization, fruit development process, plant photosynthesis which can be dugout by experiment expression validation.

4. Conclusion

The orange is considered as the second highest produced fruits all over the world. The *C.* s*inensis* plant is the major source of sweet orange which is one of the most favourite and nutritious fruits. Identification, characterization and diversity analyses of the RNAi gene families were essential, since these families play the vital role for silencing of other gene families of any plant. In this study, a number of bioinformatics approaches were used to identify, characterize and analyse the diversification, properties and biological functionality of RNAi genes in *C. sinensis*. By this ways, we identified 4 CsDCL, 8 CsAGO and 4 CsRDR genes as the RNAi gene families in sweet orange. This study also provided additional genomic and physicochemical information of the predicted genes and corresponding proteins. With the phylogenetic analysis, the subgroups of the three gene families were exhibited, the domains and motifs configuration and the gene structures revealed the maximum homogeneity with the respective gene family of Arabidopsis. Moreover, the GO enrichment and subcellular localization analysis provided the final confirmation about the reported genes and protein that, these are the key factor of RNAi process in *C. sinensis*. In this analysis, we explored regulatory relationship network between TFs and proposed RNAi genes. Potential targets of TFs were identified those involved in plant growth and development as well as controlling the gene expression or suppression related to RNAi process. The *cis*-acting regulatory elements and expressed sequence tag (EST) analysis indicates that our reported RNAi genes have diverse involvement into the orange plant growth, flowering, and development processes. Thus the reported genes in this study may exhibit significant expression pattern under different stress conditions in various developmental stages of sweet orange like the other plants that were investigated by other researchers. Therefore, the findings of this study may provide a basis for further research on RNAi pathway genes in *C. sinensis* to enrich the ultimate sweet orange plant development and fruit production all dover the world.

Supplementary Files

Supplementary datasets, tables and figures are available at www.bbcba.org/softwares/CsRNAi.zip.

Abbreviations

AGO, Argonaute; BLAST, Basic Local Alignment Search Tool; bp, base pair; DCL, Dicer-Like; GO, Gene Ontology; GSDS, Gene Structure Display Server; HMM, Hidden Markov Model; MEME, Multiple Em for Motif Elicitation; miRNA, microRNA; PTGS, post-transcriptional gene silencing ; RDR, RNA, dependent RNA polymerase ; RNAi, RNA interference;

RISC, RNA-induced silencing complex; sRNA, small RNA; siRNA, short interfering RNA; TF, transcription factor; TGS, transcriptional gene silencing.

Conflict of Interest

The authors have no conflicts of interest to declare.

Funding

This study did not receive any funds.

Supportive/supplementary legends

Supplementary Table S1: Gene location in different scaffold.

Supplementary Table S2: Sub-cellular Localization of the predicted proteins

Supplementary Table S3: Distribution of TF families those regulating RNAi genes.

Supplementary Data S1: Protein sequences of the predicted DCL genes of *Citrus sinensis.*

Supplementary Data S2: Protein sequences of the predicted AGO genes of *Citrus sinensis.*

Supplementary Data S3: Protein sequences of the predicted RDR genes of *Citrus sinensis.*

Supplementary Data S4: GO enrichment analysis result for predicted RNAi genes.

Supplementary Data S5: List of transcript factors and their families regulating predicted RNAi genes.

Supplementary Fig. S1: GO enrichment analysis of the predicted RNAi genes **(A)** biological process, **(B)** molecular function and **(C)** cellular process. In the directed acyclic graph (DAG) the downstream term corresponds to a subset of the upstream term. The significant (P < 0.05, FDR < 0.05) GO terms are in colored boxes (the degree of color saturation is positively correlated to the enrichment level of the GO term), and non-significant terms are in white boxes.

Supplementary Fig. S2: Distribution of TF families corresponding to genes. Rows of the figure represent the predicted RNAi genes and the columns represent the families of the TFs. The number indicates the TF families regulate the RNAi genes.

References

[1] Carrington, J.C. and V. Ambros, *Role of microRNAs in plant and animal development.* Science, 2003. **301**(5631): p. 336-8.

[2] Finnegan, E.J. and M.A. Matzke, *The small RNA world.* J Cell Sci, 2003. **116**(Pt 23): p. 4689-93.

[3] Lai, E.C., *microRNAs: runts of the genome assert themselves.* Curr Biol, 2003. **13**(23): p. R925-36.

[4] Wassenegger, M., et al., *RNA-directed de novo methylation of genomic sequences in plants.* Cell, 1994. **76**(3): p. 567-76.

[5] Xie, Z., et al., *Genetic and functional diversification of small RNA pathways in plants.* PLoS Biol, 2004. **2**(5): p. E104.

[6] Grosshans, H. and W. Filipowicz, *Molecular biology: the expanding world of small RNAs.* Nature, 2008. **451**(7177): p. 414-6.

[7] Chapman, E.J. and J.C. Carrington, *Specialization and evolution of endogenous small RNA pathways.* Nat Rev Genet, 2007. **8**(11): p. 884-96.

[8] Millar, A.A. and P.M. Waterhouse, *Plant and animal microRNAs: similarities and differences.* Funct Integr Genomics, 2005. **5**(3): p. 129-35.

[9] Bernstein, E., et al., *Role for a bidentate ribonuclease in the initiation step of RNA interference.* Nature, 2001. **409**(6818): p. 363-6.

[10] Hammond, S.M., et al., *Argonaute2, a link between genetic and biochemical analyses of RNAi.* Science, 2001. **293**(5532): p. 1146-50.

[11] Margis, R., et al., *The evolution and diversification of Dicers in plants.* FEBS Lett, 2006. **580**(10): p. 2442-50.

[12] Moazed, D., *Small RNAs in transcriptional gene silencing and genome defence.* Nature, 2009. **457**(7228): p. 413-20.

[13] Kapoor, M., et al., *Genome-wide identification, organization and phylogenetic analysis of Dicer-like, Argonaute and RNA-dependent RNA Polymerase gene families and their expression analysis during reproductive development and stress in rice.* BMC Genomics, 2008. **9**: p. 451.

[14] Peters, L. and G. Meister, *Argonaute proteins: mediators of RNA silencing.* Mol Cell, 2007. **26**(5): p. 611-23.

[15] Hock, J. and G. Meister, *The Argonaute protein family.* Genome Biol, 2008. **9**(2): p. 210.

[16] Yigit, E., et al., *Analysis of the C. elegans Argonaute family reveals that distinct Argonautes act sequentially during RNAi.* Cell, 2006. **127**(4): p. 747-57.

[17] Hutvagner, G. and M.J. Simard, *Argonaute proteins: key players in RNA silencing.* Nat Rev Mol Cell Biol, 2008. **9**(1): p. 22-32.

[18] Girard, A., et al., *A germline-specific class of small RNAs binds mammalian Piwi proteins.* Nature, 2006. **442**(7099): p. 199-202.

[19] Djupedal, I. and K. Ekwall, *Epigenetics: heterochromatin meets RNAi.* Cell Res, 2009. **19**(3): p. 282-95.

[20] Cogoni, C. and G. Macino, *Gene silencing in Neurospora crassa requires a protein homologous to RNA-dependent RNA polymerase.* Nature, 1999. **399**(6732): p. 166-9.

[21] Dalmay, T., et al., *An RNA-dependent RNA polymerase gene in Arabidopsis is required for posttranscriptional gene silencing mediated by a transgene but not by a virus.* Cell, 2000. **101**(5): p. 543-53.

[22] Wang, J., C. Li, and E. Wang, *Potential and flux landscapes quantify the stability and robustness of budding yeast cell cycle network.* Proc Natl Acad Sci U S A, 2010. **107**(18): p. 8195-200.

[23] Vaucheret, H., *Plant ARGONAUTES.* Trends Plant Sci, 2008. **13**(7): p. 350-8.

[24] Qian, Y., et al., *Identification and characterization of Dicer-like, Argonaute and RNA-dependent RNA polymerase gene families in maize.* Plant Cell Rep, 2011. **30**(7): p. 1347-63.

[25] Bai, M., et al., *Genome-wide identification of Dicer-like, Argonaute and RNA-dependent RNA polymerase gene families and their expression analyses in response to viral infection and abiotic stresses in Solanum lycopersicum.* Gene, 2012. **501**(1): p. 52-62.

[26] Nakasugi, K., et al., *De novo transcriptome sequence assembly and analysis of RNA silencing genes of Nicotiana benthamiana.* PLoS One, 2013. **8**(3): p. e59534.

[27] Yadav, C.B., et al., *Identification, characterization and expression profiling of Dicer-like, Argonaute and RNA-dependent RNA polymerase gene families in foxtail millet.* Plant molecular biology reporter, 2015. **33**(1): p. 43-55.

[28] Zhao, H., et al., *Comprehensive analysis of Dicer-Like, Argonaute, and RNA-dependent RNA polymerase gene families in grapevine (Vitis Vinifera).* Journal of plant growth regulation, 2015. **34**(1): p. 108-121.

[29] Gan, D., et al., *Expression analysis of argonaute, Dicer-like, and RNA-dependent RNA polymerase genes in cucumber (Cucumis sativus L.) in response to abiotic stress.* J Genet, 2017. **96**(2): p. 235-249.

[30] Qin, L., et al., *Genome-Wide Analysis of DCL, AGO, and RDR Gene Families in Pepper (Capsicum Annuum L.).* Int J Mol Sci, 2018. **19**(4).

[31] Zilberman, D., X. Cao, and S.E. Jacobsen, *ARGONAUTE4 control of locus-specific siRNA accumulation and DNA and histone methylation.* Science, 2003. **299**(5607): p. 716-9.

[32] Henderson, I.R., et al., *Dissecting Arabidopsis thaliana DICER function in small RNA processing, gene silencing and DNA methylation patterning.* Nat Genet, 2006. **38**(6): p. 721-5.

[33] Deleris, A., et al., *Hierarchical action and inhibition of plant Dicer-like proteins in antiviral defense.* Science, 2006. **313**(5783): p. 68-71.

[34] Schmitz, R.J., et al., *DICER-LIKE 1 and DICER-LIKE 3 redundantly act to promote flowering via repression of FLOWERING LOCUS C in Arabidopsis thaliana.* Genetics, 2007. **176**(2): p. 1359-62.

[35] Liu, B., et al., *Loss of function of OsDCL1 affects microRNA accumulation and causes developmental defects in rice.* Plant Physiol, 2005. **139**(1): p. 296-305.

[36] Fagard, M., et al., *AGO1, QDE-2, and RDE-1 are related proteins required for post-transcriptional gene silencing in plants, quelling in fungi, and RNA interference in animals.* Proc Natl Acad Sci U S A, 2000. **97**(21): p. 11650-4.

[37] Hunter, C., H. Sun, and R.S. Poethig, *The Arabidopsis heterochronic gene ZIPPY is an ARGONAUTE family member.* Curr Biol, 2003. **13**(19): p. 1734-9.

[38] Moussian, B., et al., *Role of the ZWILLE gene in the regulation of central shoot meristem cell fate during Arabidopsis embryogenesis.* EMBO J, 1998. **17**(6): p. 1799-809.

[39] Mourrain, P., et al., *Arabidopsis SGS2 and SGS3 genes are required for posttranscriptional gene silencing and natural virus resistance.* Cell, 2000. **101**(5): p. 533-42.

[40] Jovel, J., M. Walker, and H. Sanfacon, *Recovery of Nicotiana benthamiana plants from a necrotic response induced by a nepovirus is associated with RNA silencing but not with reduced virus titer.* J Virol, 2007. **81**(22): p. 12285-97.

[41] Matzke, M., et al., *Targets of RNA-directed DNA methylation.* Curr Opin Plant Biol, 2007. **10**(5): p. 512-9.

[42] Dorweiler, J.E., et al., *mediator of paramutation1 is required for establishment and maintenance of paramutation at multiple maize loci.* Plant Cell, 2000. **12**(11): p. 2101-18.

[43] Etebu, E. and A. Nwauzoma, *A review on sweet orange (Citrus sinensis L Osbeck): health, diseases and management.* American Journal of Research Communication, 2014. **2**(2): p. 33-70.

[44] Hertog, M.G., et al., *Dietary antioxidant flavonoids and risk of coronary heart disease: the Zutphen Elderly Study.* Lancet, 1993. **342**(8878): p. 1007-11.

[45] Crowell, P.L., *Prevention and therapy of cancer by dietary monoterpenes.* J Nutr, 1999. **129**(3): p. 775S-778S.

[46] Tripoli, E., et al., *Citrus flavonoids: Molecular structure, biological activity and nutritional properties: A review.* Food chemistry, 2007. **104**(2): p. 466-479.

[47. Di Majo, D., et al., *Flavanones in Citrus fruit: Structure–antioxidant activity relationships.* Food Research International, 2005. **38**(10): p. 1161-1166.

[48] Thompson, J.D., D.G. Higgins, and T.J. Gibson, *CLUSTAL W: improving the sensitivity of progressive multiple sequence alignment through sequence weighting, position-specific gap penalties and weight matrix choice.* Nucleic Acids Res, 1994. **22**(22): p. 4673-80.

[49] Tamura, K., et al., *MEGA5: molecular evolutionary genetics analysis using maximum likelihood, evolutionary distance, and maximum parsimony methods.* Mol Biol Evol, 2011. **28**(10): p. 2731-9.

[50] Saitou, N. and M. Nei, *The neighbor-joining method: a new method for reconstructing phylogenetic trees.* Mol Biol Evol, 1987. **4**(4): p. 406-25.

[51] Felsenstein, J., *Confidence Limits on Phylogenies: An Approach Using the Bootstrap.* Evolution, 1985. **39**(4): p. 783-791.

[52] Tajima, F. and M. Nei, *Estimation of evolutionary distance between nucleotide sequences.* Mol Biol Evol, 1984. **1**(3): p. 269-85.

[53] Bailey, T.L. and C. Elkan, *The value of prior knowledge in discovering motifs with MEME.* Proc Int Conf Intell Syst Mol Biol, 1995. **3**: p. 21-9.

[54] Jin, J., et al., *PlantTFDB 4.0: toward a central hub for transcription factors and regulatory interactions in plants.* Nucleic Acids Res, 2017. **45**(D1): p. D1040-D1045.

[55] Liu, L., et al., *PSI: a comprehensive and integrative approach for accurate plant subcellular localization prediction.* PLoS One, 2013. **8**(10): p. e75826.

[56] Shannon, P., et al., *Cytoscape: a software environment for integrated models of biomolecular interaction networks.* Genome Res, 2003. **13**(11): p. 2498-504.

[57] MacRae, I.J. and J.A. Doudna, *Ribonuclease revisited: structural insights into ribonuclease III family enzymes.* Curr Opin Struct Biol, 2007. **17**(1): p. 138-45.

[58] Nicholson, A.W., *The ribonuclease III family: forms and functions in RNA maturation, decay, and gene silencing.* RNAi: A guide to gene silencing, 2003: p. 149-174.

[59] Rivas, F.V., et al., *Purified Argonaute2 and an siRNA form recombinant human RISC.* Nat Struct Mol Biol, 2005. **12**(4): p. 340-9.

[60] Baumberger, N. and D.C. Baulcombe, *Arabidopsis ARGONAUTE1 is an RNA Slicer that selectively recruits microRNAs and short interfering RNAs.* Proc Natl Acad Sci U S A, 2005. **102**(33): p. 11928-33.

[61] Iyer, L.M., E.V. Koonin, and L. Aravind, *Evolutionary connection between the catalytic subunits of DNA-dependent RNA polymerases and eukaryotic RNA-dependent RNA polymerases and the origin of RNA polymerases.* BMC Struct Biol, 2003. **3**: p. 1.

[62] Fire, A., et al., *Potent and specific genetic interference by double-stranded RNA in Caenorhabditis elegans.* Nature, 1998. **391**(6669): p. 806-11.

[63] Lingel, A. and E. Izaurralde, *RNAi: finding the elusive endonuclease.* RNA, 2004. **10**(11): p. 1675-9.

[64] Lingel, A., et al., *Structure and nucleic-acid binding of the Drosophila Argonaute 2 PAZ domain.* Nature, 2003. **426**(6965): p. 465-9.

[65] Ma, J.B., K. Ye, and D.J. Patel, *Structural basis for overhang-specific small interfering RNA recognition by the PAZ domain.* Nature, 2004. **429**(6989): p. 318-322.

[66] Agrawal, N., et al., *RNA interference: biology, mechanism, and applications.* Microbiol Mol Biol Rev, 2003. **67**(4): p. 657-85.

[67] Chery, J., *RNA therapeutics: RNAi and antisense mechanisms and clinical applications.* Postdoc J, 2016. **4**(7): p. 35-50.

[68] Shu, Y., et al., *Genome-Wide Analysis of the AP2/ERF Superfamily Genes and their Responses to Abiotic Stress in Medicago truncatula.* Front Plant Sci, 2015. **6**: p. 1247.

[69] Wen, C.L., et al., *Identification and characterisation of Dof transcription factors in the cucumber genome.* Sci Rep, 2016. **6**: p. 23072.

[70] Venkatesh, J. and S.W. Park, *Genome-wide analysis and expression profiling of DNA-binding with one zinc finger (Dof) transcription factor family in potato.* Plant Physiol Biochem, 2015. **94**: p. 73-85.

[71] Skirycz, A., et al., *DOF transcription factor AtDof1.1 (OBP2) is part of a regulatory network controlling glucosinolate biosynthesis in Arabidopsis.* Plant J, 2006. **47**(1): p. 10-24.

[72] Skirycz, A., et al., *Transcription factor AtDOF4;2 affects phenylpropanoid metabolism in Arabidopsis thaliana.* New Phytol, 2007. **175**(3): p. 425-38.

[73] Khaled Mirzaei, Bahman Bahramnejad, Mohammad Hasan Shamsifard, and Wahid Zamani, "*In Silico Identification, Phylogenetic and Bioinformatic Analysis of Argonaute Genes in Plants*," International Journal of Genomics, vol. 2014, Article ID 967461, 17 pages, 2014. https://doi.org/10.1155/2014/967461.

Author Contribution

MPM and MNHM designed the research. MPM analyzed the data using different bioinformatics and statistical tools. MAA and MPM carried out the GO enrichment, subcellular localization and regulatory transcription factor analysis. MPM drafted and MNHM finalized the manuscript. HR, ZA, FFA, MMI and MAM attended at the meetings, presentations and discussion regarding the manuscripts. All authors read and approved the manuscript.

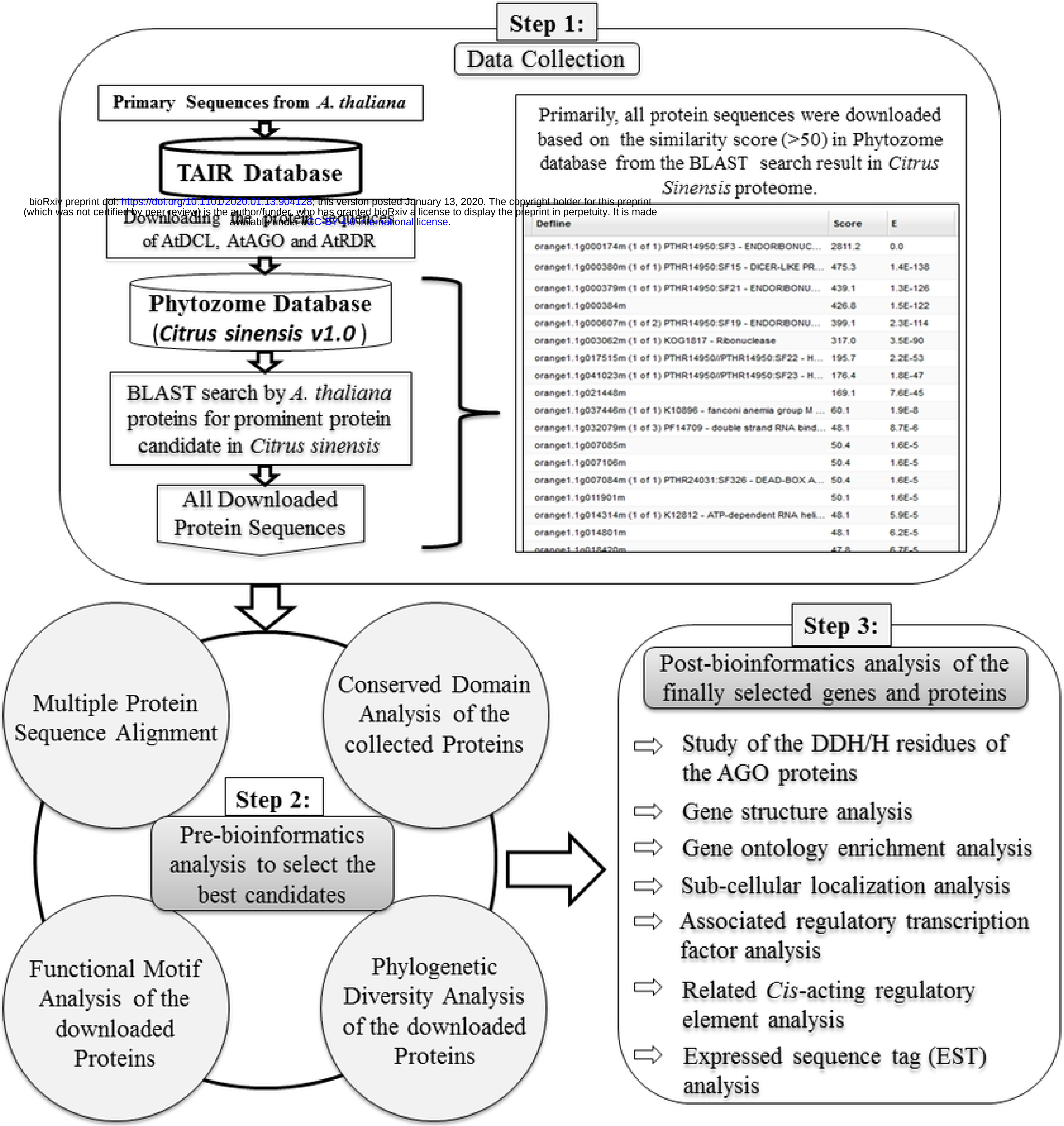

Step 1:
Data Collection

Primary Sequences from *A. thaliana*
TAIR Database
Downloading the protein sequences of AtDCL, AtAGO and AtRDR
Phytozome Database (*Citrus sinensis v1.0*)
BLAST search by *A. thaliana* proteins for prominent protein candidate in *Citrus sinensis*
All Downloaded Protein Sequences

Primarily, all protein sequences were downloaded based on the similarity score (>50) in Phytozome database from the BLAST search result in *Citrus Sinensis* proteome.

Defline	Score	E
orange1.1g000174m (1 of 1) PTHR14950:SF3 - ENDORIBONUC...	2811.2	0.0
orange1.1g000380m (1 of 1) PTHR14950:SF15 - DICER-LIKE PR...	475.3	1.4E-138
orange1.1g000379m (1 of 1) PTHR14950:SF21 - ENDORIBONU...	439.1	1.3E-126
orange1.1g000384m	426.8	1.5E-122
orange1.1g000607m (1 of 2) PTHR14950:SF19 - ENDORIBONU...	399.1	2.3E-114
orange1.1g003062m (1 of 1) KOG1817 - Ribonuclease	317.0	3.5E-90
orange1.1g017515m (1 of 1) PTHR14950//PTHR14950:SF22 - H...	195.7	2.2E-53
orange1.1g041023m (1 of 1) PTHR14950//PTHR14950:SF23 - H...	176.4	1.8E-47
orange1.1g021448m	169.1	7.6E-45
orange1.1g037446m (1 of 1) K10896 - fanconi anemia group M ...	60.1	1.9E-8
orange1.1g032079m (1 of 3) PF14709 - double strand RNA bind...	48.1	8.7E-6
orange1.1g007085m	50.4	1.6E-5
orange1.1g007106m	50.4	1.6E-5
orange1.1g007084m (1 of 1) PTHR24031:SF326 - DEAD-BOX A...	50.4	1.6E-5
orange1.1g011901m	50.1	1.6E-5
orange1.1g014314m (1 of 1) K12812 - ATP-dependent RNA heli...	48.1	5.9E-5
orange1.1g014801m	48.1	6.2E-5
orange1.1g018420m	47.8	6.7E-5

Step 2:
Pre-bioinformatics analysis to select the best candidates

Multiple Protein Sequence Alignment
Conserved Domain Analysis of the collected Proteins
Functional Motif Analysis of the downloaded Proteins
Phylogenetic Diversity Analysis of the downloaded Proteins

Step 3:
Post-bioinformatics analysis of the finally selected genes and proteins

⇨ Study of the DDH/H residues of the AGO proteins
⇨ Gene structure analysis
⇨ Gene ontology enrichment analysis
⇨ Sub-cellular localization analysis
⇨ Associated regulatory transcription factor analysis
⇨ Related *Cis*-acting regulatory element analysis
⇨ Expressed sequence tag (EST) analysis

Figure 1

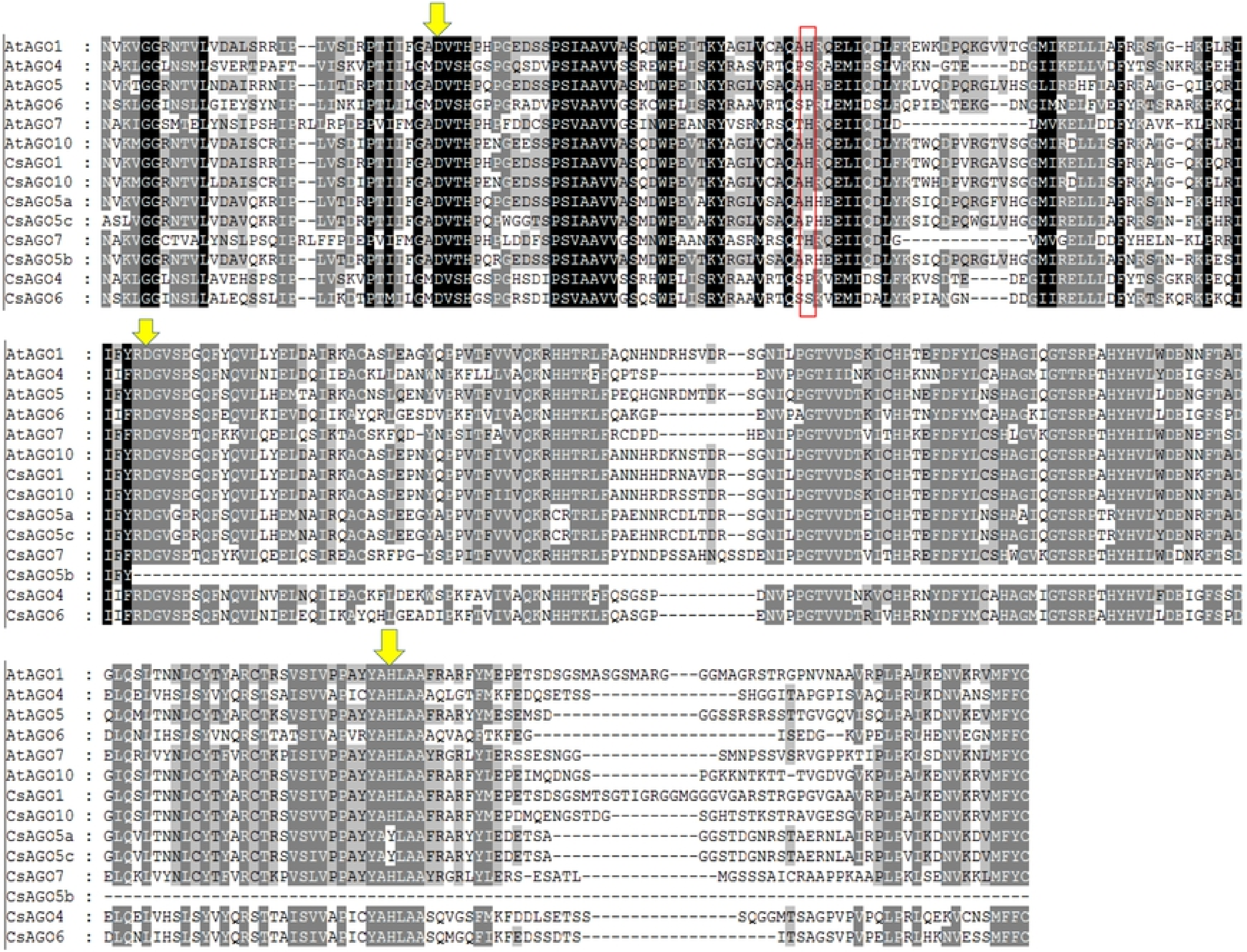

```
AtAGO1  : NVKVGGRNTVLVDALSRRIP--LVSDRPTIIFGADVTHPHPGEDSSPSIAAVVASQDWPEITKYAGLVCAQAHRQELIQDLFKEWKDPQKGVVTGGMIKELLIAFRRSTG-HKPLRI
AtAGO4  : NAKLGGLNSMLSVERTPAFT--VISKVPTIILGMDVSHGSPGQSDVPSIAAVVSSREWPLISKYRASVRTQPSKAEMIESLVKKN-GTE----DDGIIKELLVDFYTSSNKRKPEHI
AtAGO5  : NVKTGGRNTVLNDAIRRNIP--LITDRPTIIMGADVTHPQPGEDSSPSIAAVVASMDWPEINKYRGLVSAQAHREEIIQDLYKLVQDPQRGLVHSGLIREHFIAFRRATG-QIPQRI
AtAGO6  : NSKLGGINSLLGIEYSYNIP--LINKIPTLILGMDVSHGPPGRADVPSVAAVVGSKCWPLISRYRAAVRTQSPRLEMIDSLFQPIENTEKG--DNGIMNELFVEFYRTSRARKPKQI
AtAGO7  : NAKIGGSMTELYNSIPSHIPRLLRPDEPVIFMGADVTHPHPFDDCSPSVAAVVGSINWPEANRYVSRMRSQTHRQEIIQDLD-------------IMVKELLDDFYKAVK-KLPNRI
AtAGO10 : NVKMGGRNTVLVDAISCRIP--LVSDIPTIIFGADVTHPENGEESSPSIAAVVASQDWPEVTKYAGLVCAQAHRQELIQDLYKTWQDPVRGTVSGGMIRDLLISFRKATG-QKPLRI
CsAGO1  : NVKVGGRNTVLVDAISRRIP--LVSDRPTIIFGADVTHPHPGEDSSPSIAAVVASQDWPEVTKYAGLVCAQAHRQELIQDLFKTWQDPVRGAVSGGMIKELLISFRRATG-QKPQRI
CsAGO10 : NVKMGGRNTVLLDAISCRIP--LVSDIPTIIFGADVTHPENGEDSSPSIAAVVASQDWPEVTKYAGLVCAQAHRQELIQDLYKTWHDPVRGTVSGGMIRDLLISFRKATG-QKPLRI
CsAGO5a : NVKVGGRNTVLVDAVQKRIP--LVTDRPTIIFGADVTHPQPGEDSSPSIAAVVASMDWPEVAKYRGLVSAQAHHEEIIQDLYKSIQDPQRGFVHGGMIRELLIAFRRSTN-FKPHRI
CsAGO5c : ASLVGGRNTVLVDAVQKRIP--LVTDRPTIIFGADVTHPQPWGGTSPSIAAVVASMDWPEVAKYRGLVSAQAPHEEIIQDLYKSIQDPQWGLVHGGMIRELLIAFRRSTN-FKPHRI
CsAGO7  : NAKVGGCTVALYNSLPSQIPRLFFPDEPVIFMGADVTHPHPLDDFSPSVAAVVGSMNWPAANKYASRMRSQTHRQEIIQDLG-------------VMVGELLDDFYHELN-KLPRRI
CsAGO5b : NVKVGGRNTVLVDAVQKRIP--LVTDRPTIIFGADVTHPQRGEDSSPSIAAVVASMDWPEVTKYRGLVSAQARHEEIIQDLYKSIQDPQRGLVHGGMIRELLIAFNRSTN-RKPESI
CsAGO4  : NAKLGGLNSLLAVEHSPSIP--IVSKVPTIILGMDVSHGSPGHSDIPSIAAVVSSRHWPLISRYRAAVRTQSPKVEMIDSLFKKVSDTE----DEGIIRELLLDFYTSSGKRKPEQI
CsAGO6  : NSKLGGINSLLALEQSSLIP--LIKDTPTMILGMDVSHGSPGRSDIPSVAAVVGSQSWPLISRYRAAVRTQSSKVEMIDALYKPIANGN----DDGIIRELLLDFYRTSKQRKPKQI

AtAGO1  : IFYRDGVSEGQFYQVLLYELDAIRKACASLEAGYQPPVTFVVVQKRHHTRLFAQNHNDRHSVDR--SGNILPGTVVDSKICHPTEFDFYLCSHAGIQGTSRPAHYHVLWDENNFTAD
AtAGO4  : IIFRDGVSESQFNQVLNIELDQIIEACKLLDANWNPKFLLLVAQKNHHTKFFQPTSP----------ENVPPGTIIDNKICHPKNNDFYLCAHAGMIGTTRPTHYHVLYDEIGFSAD
AtAGO5  : IFYRDGVSEGQFSQVLLHEMTAIRKACNSLQENYVPRVTFVIVQKRHHTRLFPEQHGNRDMTDK--SGNIQPGTVVDTKICHPNEFDFYLNSHAGIQGTSRPAHYHVLLDENGFTAD
AtAGO6  : IIFRDGVSESQFEQVLKIEVDQIIKAYQRLGESDVPKFTVIVAQKNHHTKLFQAKGP----------ENVPAGTVVDTKIVHPTNYDFYMCAHAGKIGTSRPAHYHVLLDEIGFSPD
AtAGO7  : IFFRDGVSETQFKKVLQEELQSIKTACSKFQD-YNPSITFAVVQKRHHTRLFRCDPD---------HENIPPGTVVDTVITHPKEFDFYLCSHLGVKGTSRPTHYHILWDENEFTSD
AtAGO10 : IFYRDGVSEGQFYQVLLYELDAIRKACASLEPNYQPPVTFIVVQKRHHTRLFANNHRDKNSTDR--SGNILPGTVVDTKICHPTEFDFYLCSHAGIQGTSRPAHYHVLWDENNFTAD
CsAGO1  : IFYRDGVSEGQFYQVLLYELDAIRKACASLEPNYQPPVTFVVVQKRHHTRLFANNHHDRNAVDR--SGNILPGTVVDSKICHPTEFDFYLCSHAGIQGTSRPAHYHVLWDENKFTAD
CsAGO10 : IFYRDGVSEGQFYQVLLYELDAIRKACASLEPNYQPPVTFIIVQKRHHTRLFANNHRDRSSTDR--SGNILPGTVVDSKICHPTEFDFYLCSHAGIQGTSRPAHYHVLWDENNFTAD
CsAGO5a : IFYRDGVGERQFSQVLLHEMNAIRQACASLEEGYAPPVTFVVVQKRCRTRLFPAENNRCDLTDR--SGNILPGTVVDTEICHPTEFDFYLNSHAAIQGTSRPTRYHVLYDENRFTAD
CsAGO5c : IFYRDGVGERQFSQVLLHEMNAIRQACASLEEGYAPPVTFVVVQKRCRTRLFPAEHNRCDLTDR--SGNILPGTVVDTEICHPTEFDFYLNSHAGIQGTSRPTRYHVLYDENRFTAD
CsAGO7  : IFFRDGVSETQFYKVLQEELQSIREACSRFPG-YSPPITFVVVQKRHHTRLFPYDNDPSSAHNQSSDENIPPGTVVDTVITHPREFDFYLCSHWGVKGTSRPTHYHILWDDNKFTSD
CsAGO5b : IFY------------------------------------------------------------------------------------------------------------------
CsAGO4  : IIFRDGVSESQFNQVLNVELNQIIEACKFLDEKWSPKFAVIVAQKNHHTKFFQSGSP----------DNVPPGTVVDNKVCHPRNYDFYLCAHAGMIGTSRPTHYHVLFDEIGFSSD
CsAGO6  : IIFRDGVSESQFNQVLNIELEQIIKAYQHLGEADIPKFTVIVAQKNHHTKLFQASGP----------ENVPPGTVVDTRIVHPRNYDFYMCAHAGMIGTSRPAHYHVLLDEIGFSPD

AtAGO1  : GLQSLTNNLCYTYARCTRSVSIVPPAYYAHLAAFRARFYMEPETSDSGSMASGSMARG---GGMAGRSTRGPNVNAAVRPLPALKENVKRVMFYC
AtAGO4  : ELQELVHSLSYVYQRSTSAISVVAPICYAHLAAAQLGTFMKFEDQSETSS---------------SHGGITAPGPISVAQLPRLKDNVANSMFFC
AtAGO5  : QLQMLTNNLCYTYARCTKSVSIVPPAYYAHLAAFRARYYMESEMSD---------------GGSSRSRSSTTGVGQVISQLPAIKDNVKEVMFYC
AtAGO6  : DLQNLIHSLSYVNQRSTTATSIVAPVRYAHLAAAQVAQFTKFEG-------------------------ISEDG--KVPELPRLHENVEGNMFFC
AtAGO7  : ELQRLVYNLCYTFVRCTKPISIVPPAYYAHLAAYRGRLYIERSSESNGG--------------SMNPSSVSRVGPPKTIPLPKLSDNVKNLMFYC
AtAGO10 : GIQSLTNNLCYTYARCTRSVSIVPPAYYAHLAAFRARFYLEPEIMQDNGS-----------PGKKNTKTT-TVGDVGVKPLPALKENVKRVMFYC
CsAGO1  : GLQSLTNNLCYTYARCTRSVSIVPPAYYAHLAAFRARFYMEPETSDSGSMTSGTIGRGGMGGGVGARSTRGPGVGAAVRPLPALKENVKRVMFYC
CsAGO10 : GIQSLTNNLCYTYARCTRSVSVVPPAYYAHLAAFRARFYMEPDMQENGSTDG---------SGHTSTKSTRAVGESGVRPLPALKENVKRVMFYC
CsAGO5a : GLQVLTNNLCYTYARCTRSVSVVPPAYYAYLAAFRARYYIEDETSA---------------GGSTDGNRSTAERNLAIRPLPVIKDNVKDVMFYC
CsAGO5c : GLQVLTNNLCYTYARCTRSVSIVPPAYYAYLAAFRARYYIEDETSA---------------GGSTDGNRSTAERNLAIRPLPVIKDNVKDVMFYC
CsAGO7  : ELQKLVYNLCYTFVRCTKPVSLVPPAYYAHLAAYRGRLYLERS-ESATL--------------MGSSSAICRAAPPKAAPLPKISENVKKLMFYC
CsAGO5b : -----------------------------------------------------------------------------------------------
CsAGO4  : ELQELVHSLSYVYQRSTTAISVVAPICYAHLAASQVGSFMKFDDLSETSS---------------SQGGMTSAGPVPVPQLPRIQEKVCNSMFFC
CsAGO6  : DLQNLIHSLSYVYQRSTTAISIVAPICYAHLAASQMGQFIKFEDSSDTS--------------------ITSAGSVPVPELPRLHKNVESSMFFC
```

Figure 2

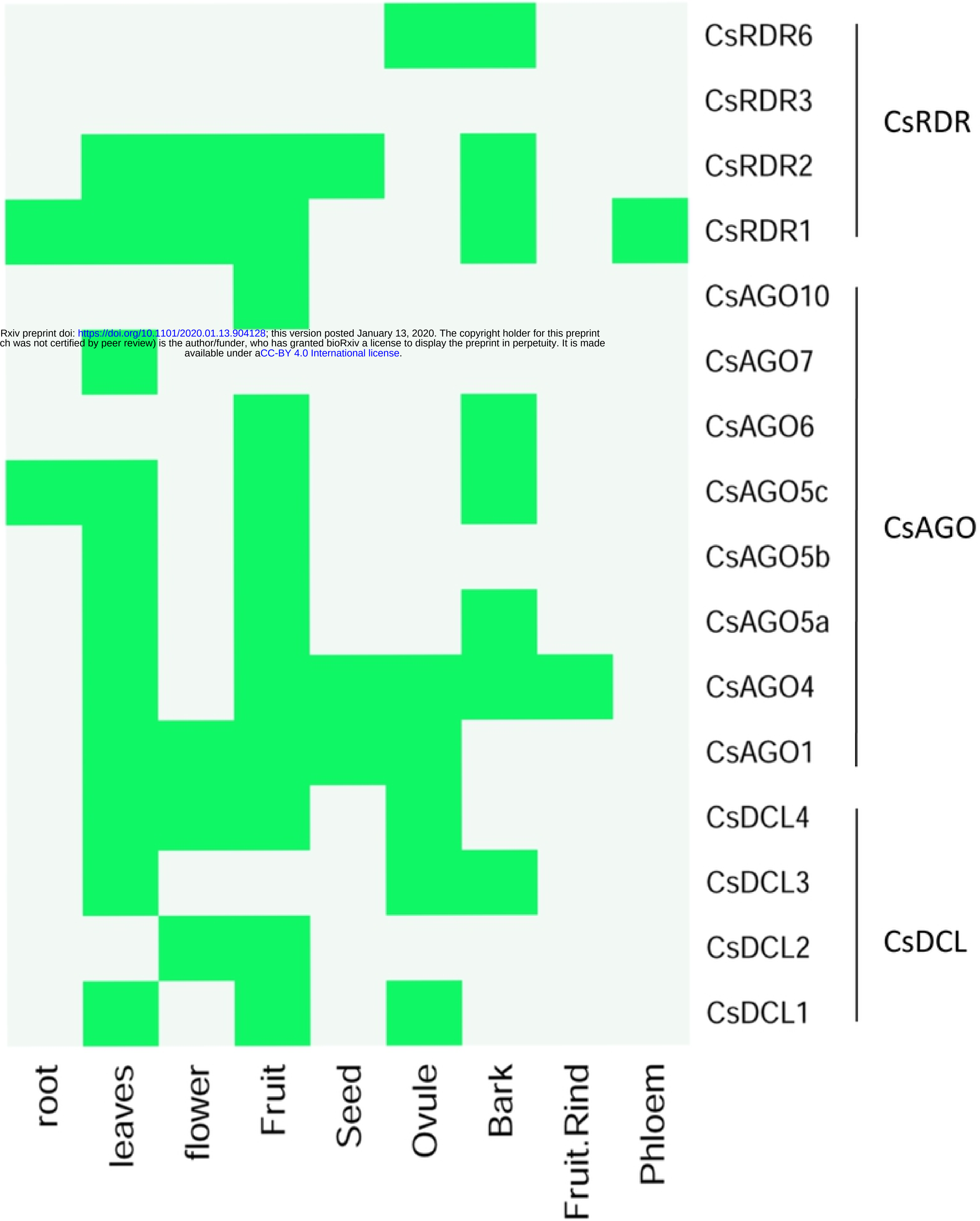
CsRDR6
CsRDR3
CsRDR2
CsRDR1
CsRDR
CsAGO10
CsAGO7
CsAGO6
CsAGO5c
CsAGO5b
CsAGO5a
CsAGO4
CsAGO1
CsAGO
CsDCL4
CsDCL3
CsDCL2
CsDCL1
CsDCL
root
leaves
flower
Fruit
Seed
Ovule
Bark
Fruit.Rind
Phloem

Figure 11

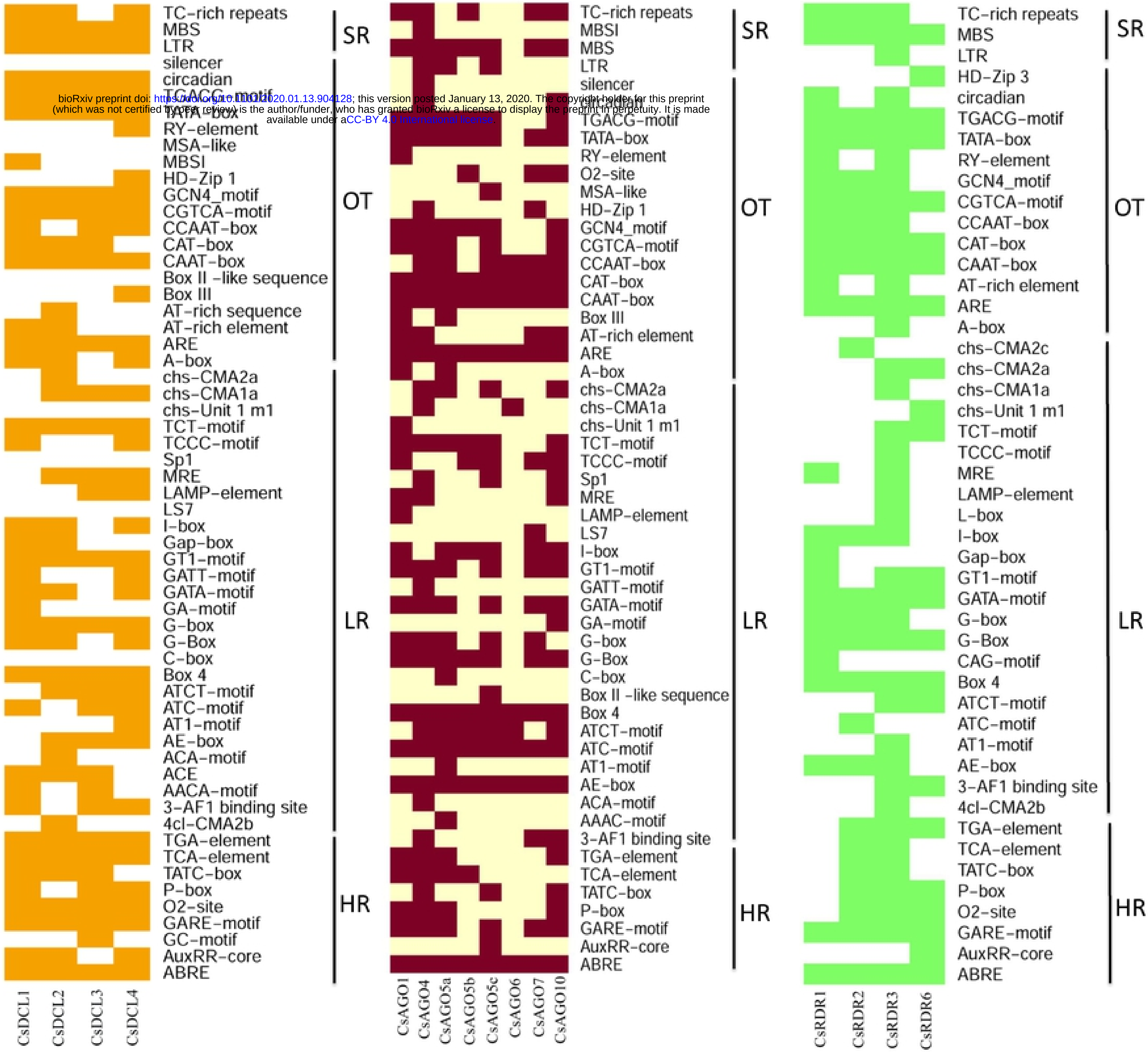
TC-rich repeats
MBS
LTR
silencer
circadian
TGACG-motif
TATA-box
RY-element
MSA-like
MBSI
HD-Zip 1
GCN4_motif
CGTCA-motif
CCAAT-box
CAT-box
CAAT-box
Box II -like sequence
Box III
AT-rich sequence
AT-rich element
ARE
A-box
chs-CMA2a
chs-CMA1a
chs-Unit 1 m1
TCT-motif
TCCC-motif
Sp1
MRE
LAMP-element
LS7
I-box
Gap-box
GT1-motif
GATT-motif
GATA-motif
GA-motif
G-box
G-Box
C-box
Box 4
ATCT-motif
ATC-motif
AT1-motif
AE-box
ACA-motif
ACE
AACA-motif
3-AF1 binding site
4cl-CMA2b
TGA-element
TCA-element
TATC-box
P-box
O2-site
GARE-motif
GC-motif
AuxRR-core
ABRE
SR
OT
LR
HR
CsDCL1
CsDCL2
CsDCL3
CsDCL4
TC-rich repeats
MBSI
MBS
LTR
silencer
circadian
TGACG-motif
TATA-box
RY-element
O2-site
MSA-like
HD-Zip 1
GCN4_motif
CGTCA-motif
CCAAT-box
CAT-box
CAAT-box
Box III
AT-rich element
ARE
A-box
chs-CMA2a
chs-CMA1a
chs-Unit 1 m1
TCT-motif
TCCC-motif
Sp1
MRE
LAMP-element
LS7
I-box
GT1-motif
GATT-motif
GATA-motif
GA-motif
G-box
G-Box
C-box
Box II -like sequence
Box 4
ATCT-motif
ATC-motif
AT1-motif
AE-box
ACA-motif
AAAC-motif
3-AF1 binding site
TGA-element
TCA-element
TATC-box
P-box
GARE-motif
AuxRR-core
ABRE
SR
OT
LR
HR
CsAGO1
CsAGO4
CsAGO5a
CsAGO5b
CsAGO5c
CsAGO6
CsAGO7
CsAGO10
TC-rich repeats
MBS
LTR
HD-Zip 3
circadian
TGACG-motif
TATA-box
RY-element
GCN4_motif
CGTCA-motif
CCAAT-box
CAT-box
CAAT-box
AT-rich element
ARE
A-box
chs-CMA2c
chs-CMA2a
chs-CMA1a
chs-Unit 1 m1
TCT-motif
TCCC-motif
MRE
LAMP-element
L-box
I-box
Gap-box
GT1-motif
GATA-motif
G-box
G-Box
CAG-motif
Box 4
ATCT-motif
ATC-motif
AT1-motif
AE-box
3-AF1 binding site
4cl-CMA2b
TGA-element
TCA-element
TATC-box
P-box
O2-site
GARE-motif
AuxRR-core
ABRE
SR
OT
LR
HR
CsRDR1
CsRDR2
CsRDR3
CsRDR6

Figure 12

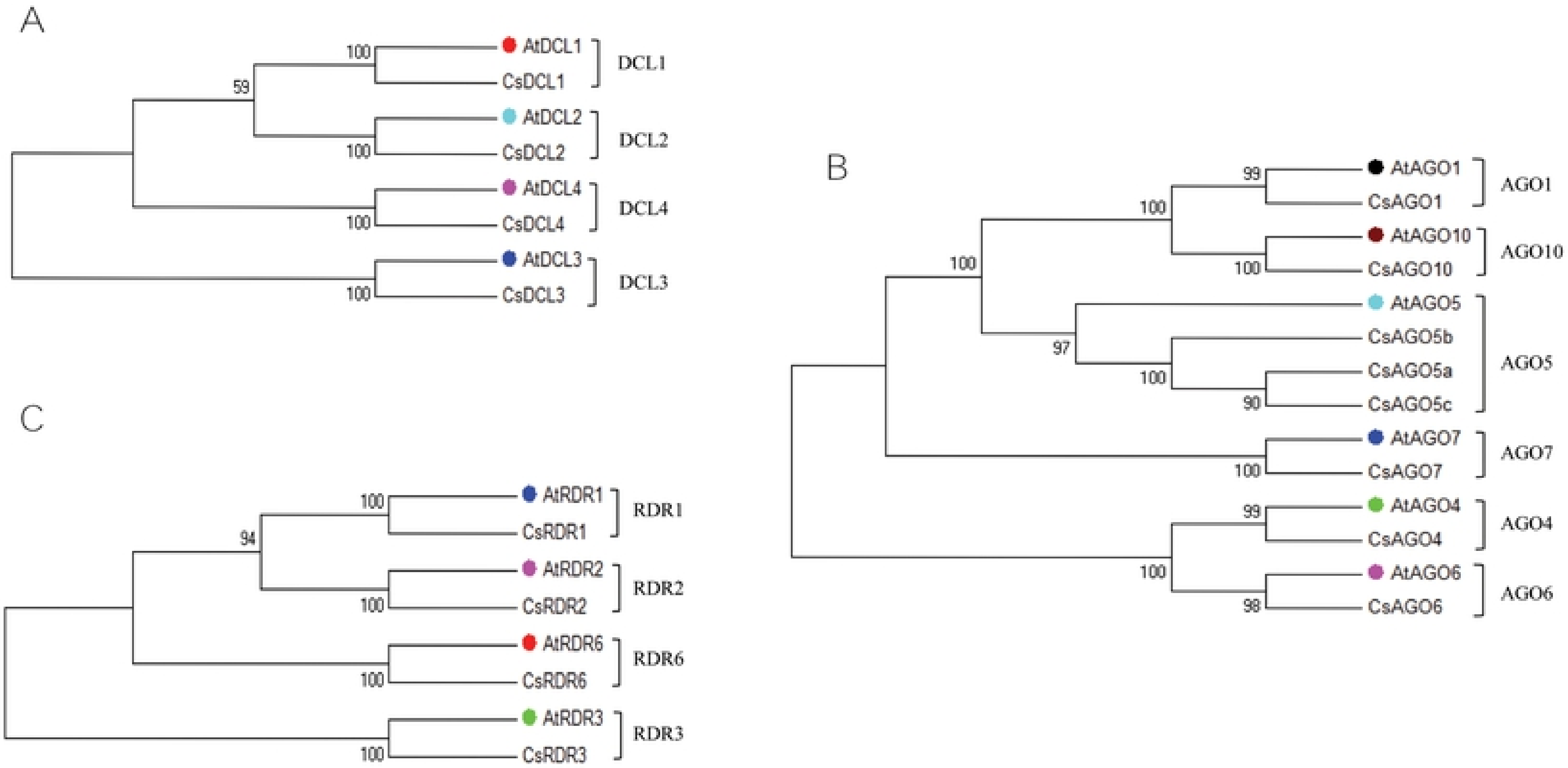
A
100
59
AtDCL1
CsDCL1
DCL1
AtDCL2
100
CsDCL2
DCL2
AtDCL4
100
CsDCL4
DCL4
AtDCL3
100
CsDCL3
DCL3
B
99
AtAGO1
CsAGO1
AGO1
100
100
AtAGO10
100
CsAGO10
AGO10
AtAGO5
CsAGO5b
97
CsAGO5a
100
90
CsAGO5c
AGO5
AtAGO7
100
CsAGO7
AGO7
99
AtAGO4
CsAGO4
AGO4
100
AtAGO6
98
CsAGO6
AGO6
C
100
AtRDR1
94
CsRDR1
RDR1
AtRDR2
100
CsRDR2
RDR2
AtRDR6
100
CsRDR6
RDR6
AtRDR3
100
CsRDR3
RDR3

Figure 3

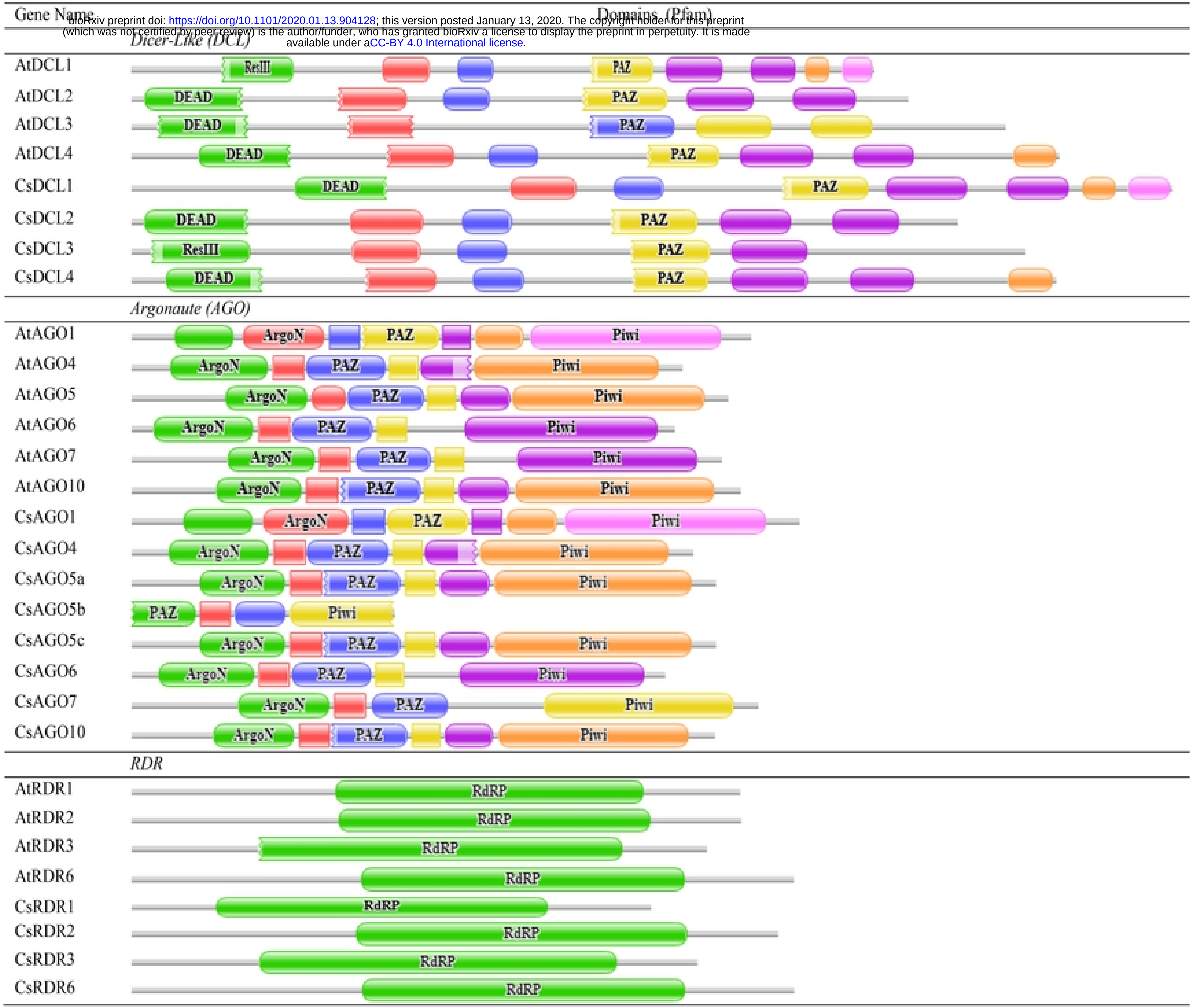
Gene Name
Domains (Pfam)
Dicer-Like (DCL)
AtDCL1 ResIII PAZ
AtDCL2 DEAD PAZ
AtDCL3 DEAD PAZ
AtDCL4 DEAD PAZ
CsDCL1 DEAD PAZ
CsDCL2 DEAD PAZ
CsDCL3 ResIII PAZ
CsDCL4 DEAD PAZ
Argonaute (AGO)
AtAGO1 ArgoN PAZ Piwi
AtAGO4 ArgoN PAZ Piwi
AtAGO5 ArgoN PAZ Piwi
AtAGO6 ArgoN PAZ Piwi
AtAGO7 ArgoN PAZ Piwi
AtAGO10 ArgoN PAZ Piwi
CsAGO1 ArgoN PAZ Piwi
CsAGO4 ArgoN PAZ Piwi
CsAGO5a ArgoN PAZ Piwi
CsAGO5b PAZ Piwi
CsAGO5c ArgoN PAZ Piwi
CsAGO6 ArgoN PAZ Piwi
CsAGO7 ArgoN PAZ Piwi
CsAGO10 ArgoN PAZ Piwi
RDR
AtRDR1 RdRP
AtRDR2 RdRP
AtRDR3 RdRP
AtRDR6 RdRP
CsRDR1 RdRP
CsRDR2 RdRP
CsRDR3 RdRP
CsRDR6 RdRP

Figure 4

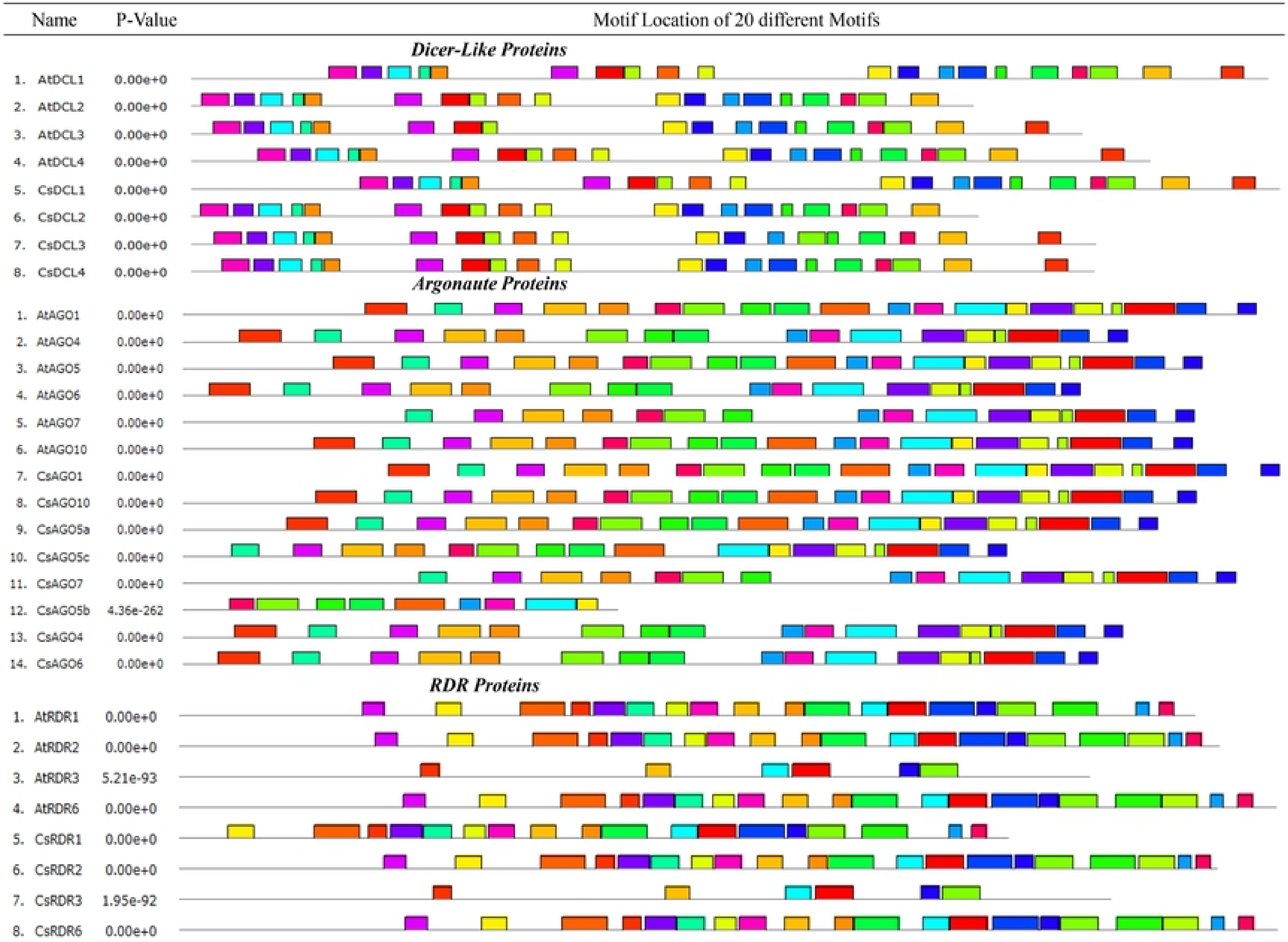
Name
P-Value
Motif Location of 20 different Motifs
Dicer-Like Proteins
1. AtDCL1 0.00e+0
2. AtDCL2 0.00e+0
3. AtDCL3 0.00e+0
4. AtDCL4 0.00e+0
5. CsDCL1 0.00e+0
6. CsDCL2 0.00e+0
7. CsDCL3 0.00e+0
8. CsDCL4 0.00e+0
Argonaute Proteins
1. AtAGO1 0.00e+0
2. AtAGO4 0.00e+0
3. AtAGO5 0.00e+0
4. AtAGO6 0.00e+0
5. AtAGO7 0.00e+0
6. AtAGO10 0.00e+0
7. CsAGO1 0.00e+0
8. CsAGO10 0.00e+0
9. CsAGO5a 0.00e+0
10. CsAGO5c 0.00e+0
11. CsAGO7 0.00e+0
12. CsAGO5b 4.36e-262
13. CsAGO4 0.00e+0
14. CsAGO6 0.00e+0
RDR Proteins
1. AtRDR1 0.00e+0
2. AtRDR2 0.00e+0
3. AtRDR3 5.21e-93
4. AtRDR6 0.00e+0
5. CsRDR1 0.00e+0
6. CsRDR2 0.00e+0
7. CsRDR3 1.95e-92
8. CsRDR6 0.00e+0

Figure 5

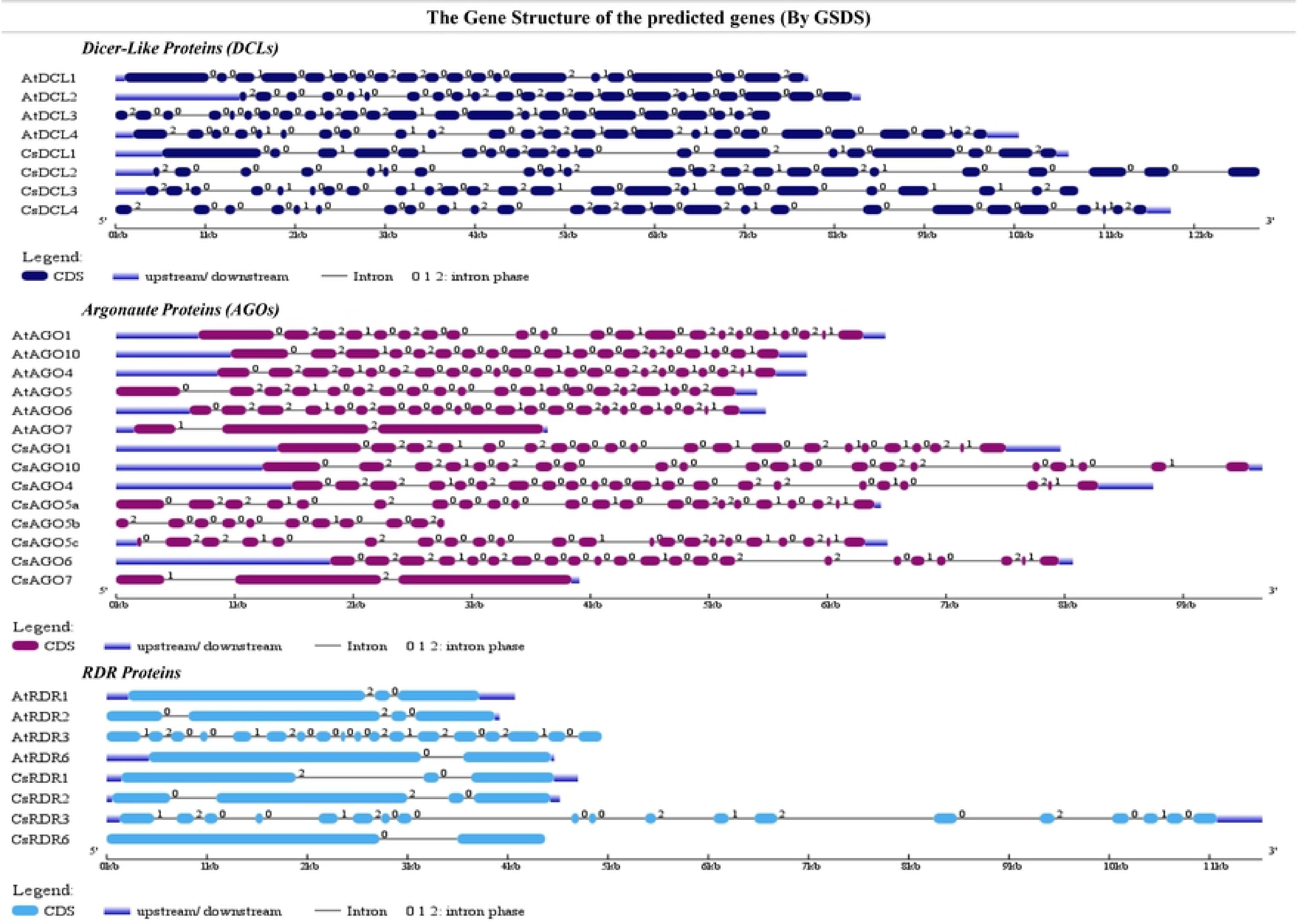
The Gene Structure of the predicted genes (By GSDS)
Dicer-Like Proteins (DCLs)
AtDCL1
AtDCL2
AtDCL3
AtDCL4
CsDCL1
CsDCL2
CsDCL3
CsDCL4
5'
3'
0kb
1kb
2kb
3kb
4kb
5kb
6kb
7kb
8kb
9kb
10kb
11kb
12kb
Legend:
CDS
upstream/ downstream
Intron
0 1 2: intron phase
Argonaute Proteins (AGOs)
AtAGO1
AtAGO10
AtAGO4
AtAGO5
AtAGO6
AtAGO7
CsAGO1
CsAGO10
CsAGO4
CsAGO5a
CsAGO5b
CsAGO5c
CsAGO6
CsAGO7
5'
3'
0kb
1kb
2kb
3kb
4kb
5kb
6kb
7kb
8kb
9kb
Legend:
CDS
upstream/ downstream
Intron
0 1 2: intron phase
RDR Proteins
AtRDR1
AtRDR2
AtRDR3
AtRDR6
CsRDR1
CsRDR2
CsRDR3
CsRDR6
5'
3'
0kb
1kb
2kb
3kb
4kb
5kb
6kb
7kb
8kb
9kb
10kb
11kb
Legend:
CDS
upstream/ downstream
Intron
0 1 2: intron phase

Figure 6

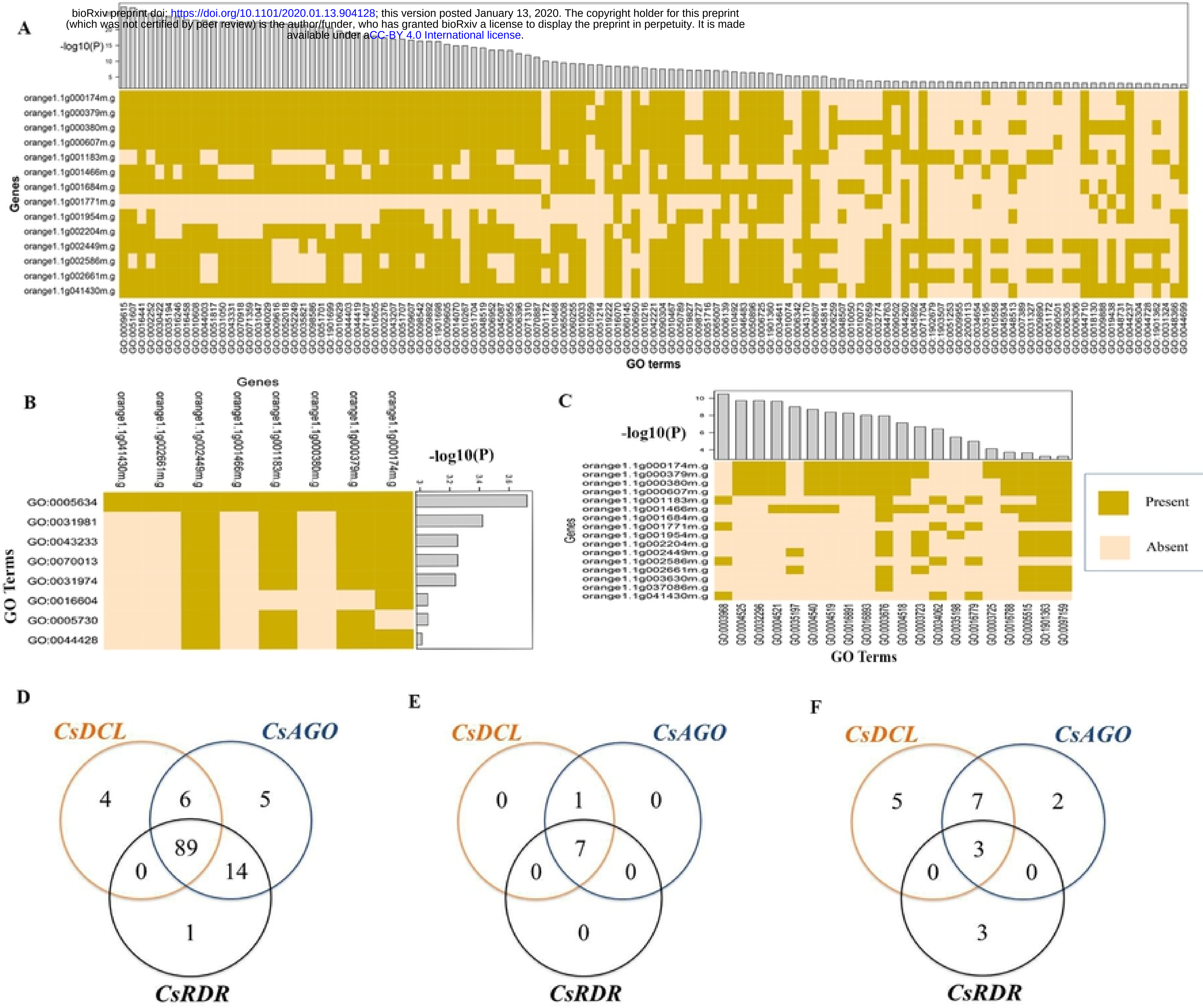
A
-log10(P)
15
10
5
Genes
orange1.1g000174m.g
orange1.1g000379m.g
orange1.1g000380m.g
orange1.1g000607m.g
orange1.1g001183m.g
orange1.1g001466m.g
orange1.1g001684m.g
orange1.1g001771m.g
orange1.1g001954m.g
orange1.1g002204m.g
orange1.1g002449m.g
orange1.1g002586m.g
orange1.1g002661m.g
orange1.1g041430m.g
GO:0009615
GO:0051607
GO:0016441
GO:0030422
GO:0035194
GO:0016246
GO:0016458
GO:0010608
GO:0044403
GO:0051817
GO:0043331
GO:0070918
GO:0071359
GO:0031047
GO:0040029
GO:0009616
GO:0052018
GO:0052249
GO:0035821
GO:0098586
GO:0051701
GO:1901699
GO:0010629
GO:0044403
GO:0044419
GO:0071407
GO:0010605
GO:0023052
GO:0043207
GO:0051707
GO:0009607
GO:0098542
GO:1901698
GO:0009892
GO:0009605
GO:0140070
GO:0010267
GO:0051704
GO:0048519
GO:0009952
GO:0045087
GO:0006955
GO:0006396
GO:0071310
GO:0070887
GO:0031172
GO:0010468
GO:0065008
GO:0060255
GO:0010033
GO:0010599
GO:0051214
GO:0019222
GO:0016070
GO:0080145
GO:0009850
GO:0010216
GO:0042221
GO:0090304
GO:0010467
GO:0050789
GO:0098727
GO:0051716
GO:0065007
GO:0006139
GO:0010492
GO:0046483
GO:0050896
GO:0006725
GO:1901360
GO:0034641
GO:0010074
GO:0019342
GO:0043170
GO:0006807
GO:0045814
GO:0065259
GO:0048507
GO:0010050
GO:0010073
GO:0097659
GO:0032774
GO:0044763
GO:0040008
GO:0044260
GO:0045892
GO:0071704
GO:1902679
GO:1903507
GO:0051253
GO:2000113
GO:0009955
GO:0034654
GO:0035196
GO:0010558
GO:0045934
GO:0048513
GO:0007389
GO:0031327
GO:0009890
GO:0051172
GO:0090501
GO:0006305
GO:0006306
GO:0044710
GO:0018130
GO:0009889
GO:0019438
GO:0048731
GO:0044237
GO:0006304
GO:0044728
GO:1901362
GO:0031324
GO:0048366
GO:0044699
GO terms
B
Genes
orange1.1g041430m.g
orange1.1g002661m.g
orange1.1g002449m.g
orange1.1g001466m.g
orange1.1g001183m.g
orange1.1g000380m.g
orange1.1g000379m.g
orange1.1g000174m.g
-log10(P)
3
3.2
3.4
3.6
GO Terms
GO:0005634
GO:0031981
GO:0043233
GO:0070013
GO:0031974
GO:0016604
GO:0005730
GO:0044428
C
-log10(P)
10
8
6
4
Genes
orange1.1g000174m.g
orange1.1g000379m.g
orange1.1g000380m.g
orange1.1g000607m.g
orange1.1g001183m.g
orange1.1g001466m.g
orange1.1g001684m.g
orange1.1g001771m.g
orange1.1g001954m.g
orange1.1g002204m.g
orange1.1g002449m.g
orange1.1g002586m.g
orange1.1g002661m.g
orange1.1g003630m.g
orange1.1g037086m.g
orange1.1g041430m.g
GO:0003968
GO:0004525
GO:0032296
GO:0004521
GO:0035197
GO:0004540
GO:0004519
GO:0016891
GO:0016893
GO:0003676
GO:0004518
GO:0003723
GO:0034062
GO:0035198
GO:0016779
GO:0003725
GO:0016788
GO:0005515
GO:1901363
GO:0097159
GO Terms
Present
Absent
D
CsDCL
CsAGO
CsRDR
4
6
5
89
0
14
1
E
CsDCL
CsAGO
CsRDR
0
1
0
7
0
0
0
F
CsDCL
CsAGO
CsRDR
5
7
2
3
0
0
3

Figure 7

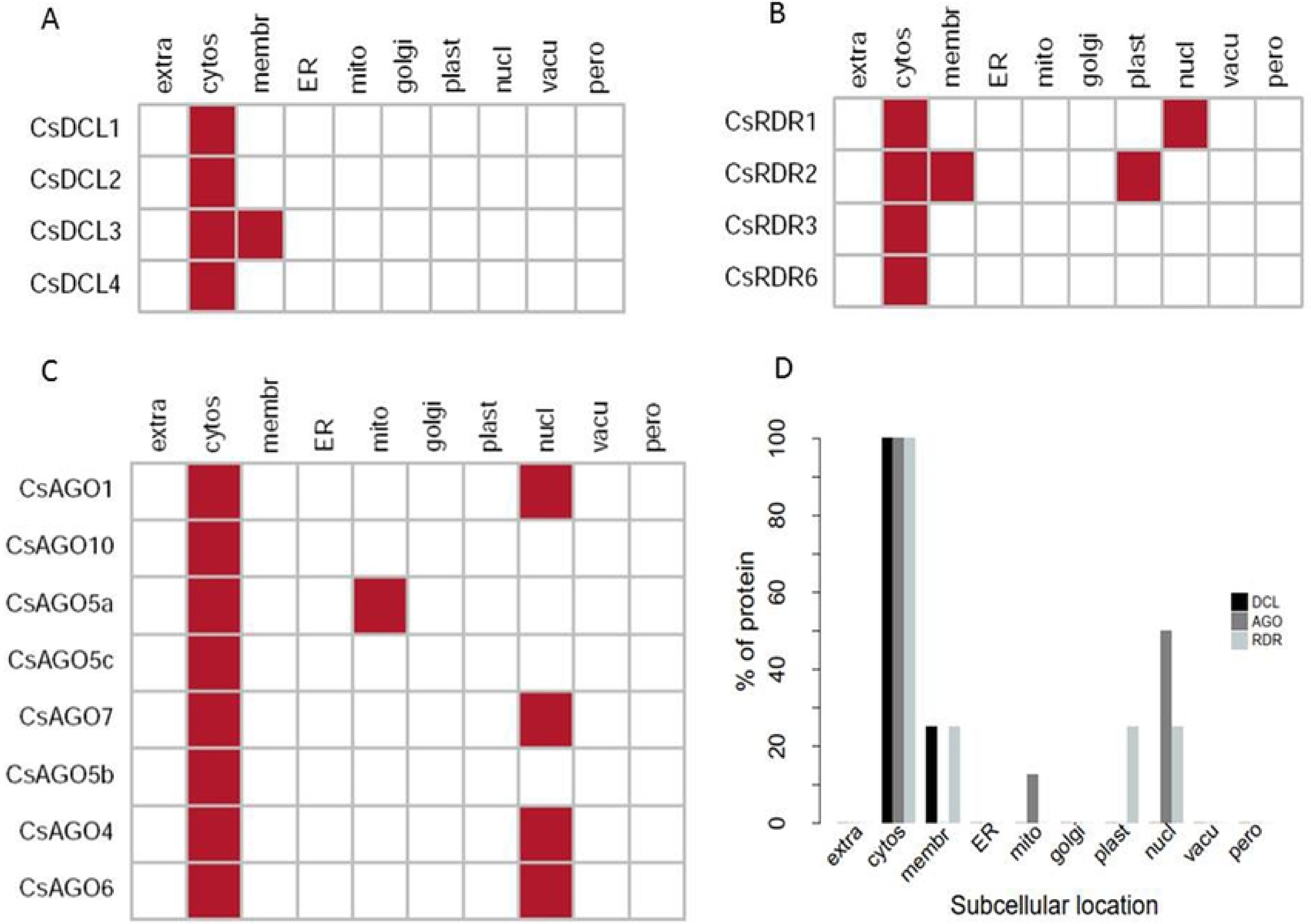
A
extra
cytos
membr
ER
mito
golgi
plast
nucl
vacu
pero
CsDCL1
CsDCL2
CsDCL3
CsDCL4
B
extra
cytos
membr
ER
mito
golgi
plast
nucl
vacu
pero
CsRDR1
CsRDR2
CsRDR3
CsRDR6
C
extra
cytos
membr
ER
mito
golgi
plast
nucl
vacu
pero
CsAGO1
CsAGO10
CsAGO5a
CsAGO5c
CsAGO7
CsAGO5b
CsAGO4
CsAGO6
D
% of protein
0
20
40
60
80
100
DCL
AGO
RDR
extra
cytos
membr
ER
mito
golgi
plast
nucl
vacu
pero
Subcellular location

Figure 8

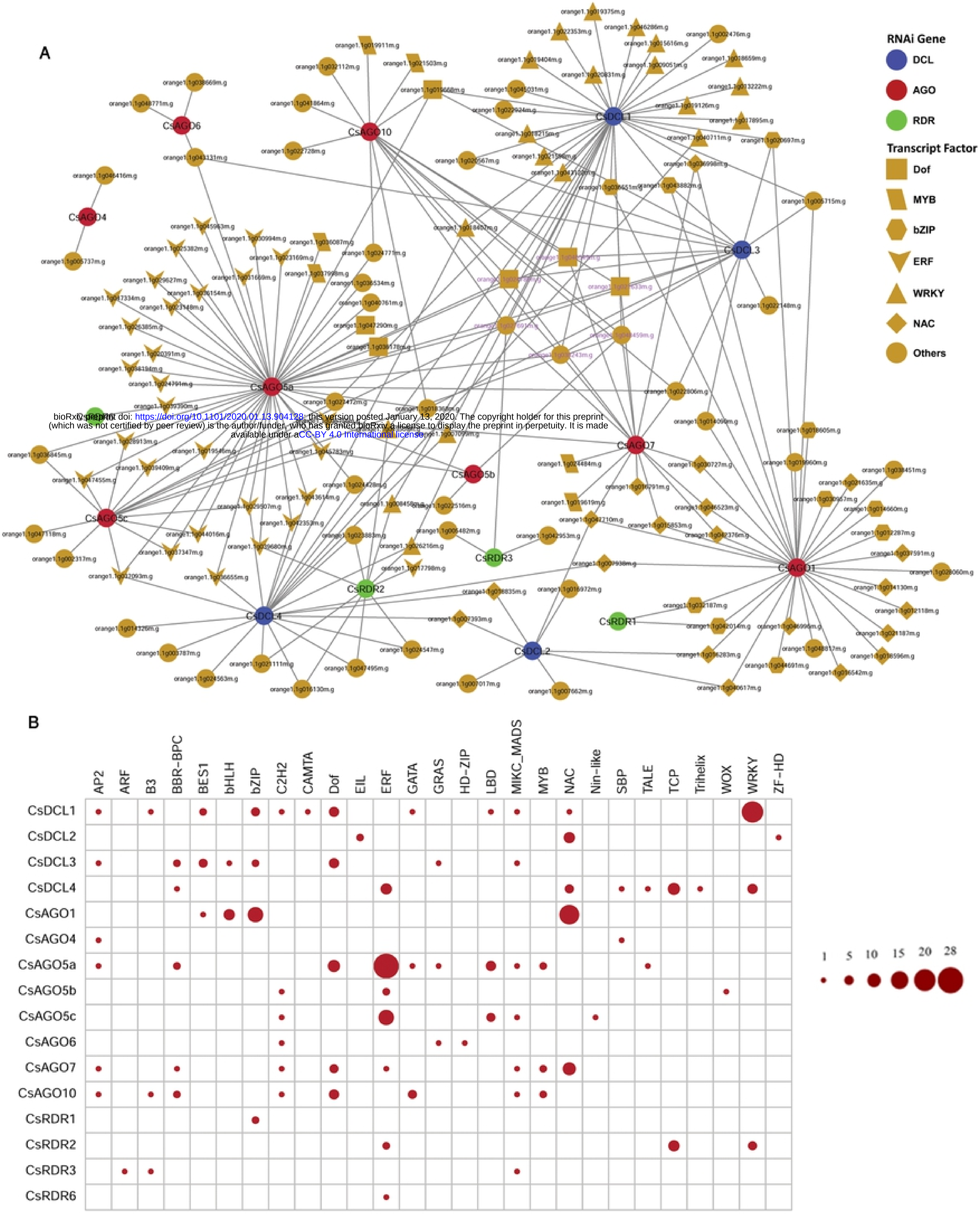
A
RNAi Gene
DCL
AGO
RDR
Transcript Factor
Dof
MYB
bZIP
ERF
WRKY
NAC
Others
CsDCL1
CsDCL2
CsDCL3
CsDCL4
CsAGO1
CsAGO4
CsAGO5a
CsAGO5b
CsAGO5c
CsAGO6
CsAGO7
CsAGO10
CsRDR1
CsRDR2
CsRDR3
B
AP2
ARF
B3
BBR−BPC
BES1
bHLH
bZIP
C2H2
CAMTA
Dof
EIL
ERF
GATA
GRAS
HD−ZIP
LBD
MIKC_MADS
MYB
NAC
Nin−like
SBP
TALE
TCP
Trihelix
WOX
WRKY
ZF−HD
CsDCL1
CsDCL2
CsDCL3
CsDCL4
CsAGO1
CsAGO4
CsAGO5a
CsAGO5b
CsAGO5c
CsAGO6
CsAGO7
CsAGO10
CsRDR1
CsRDR2
CsRDR3
CsRDR6
1
5
10
15
20
28

Figure 9

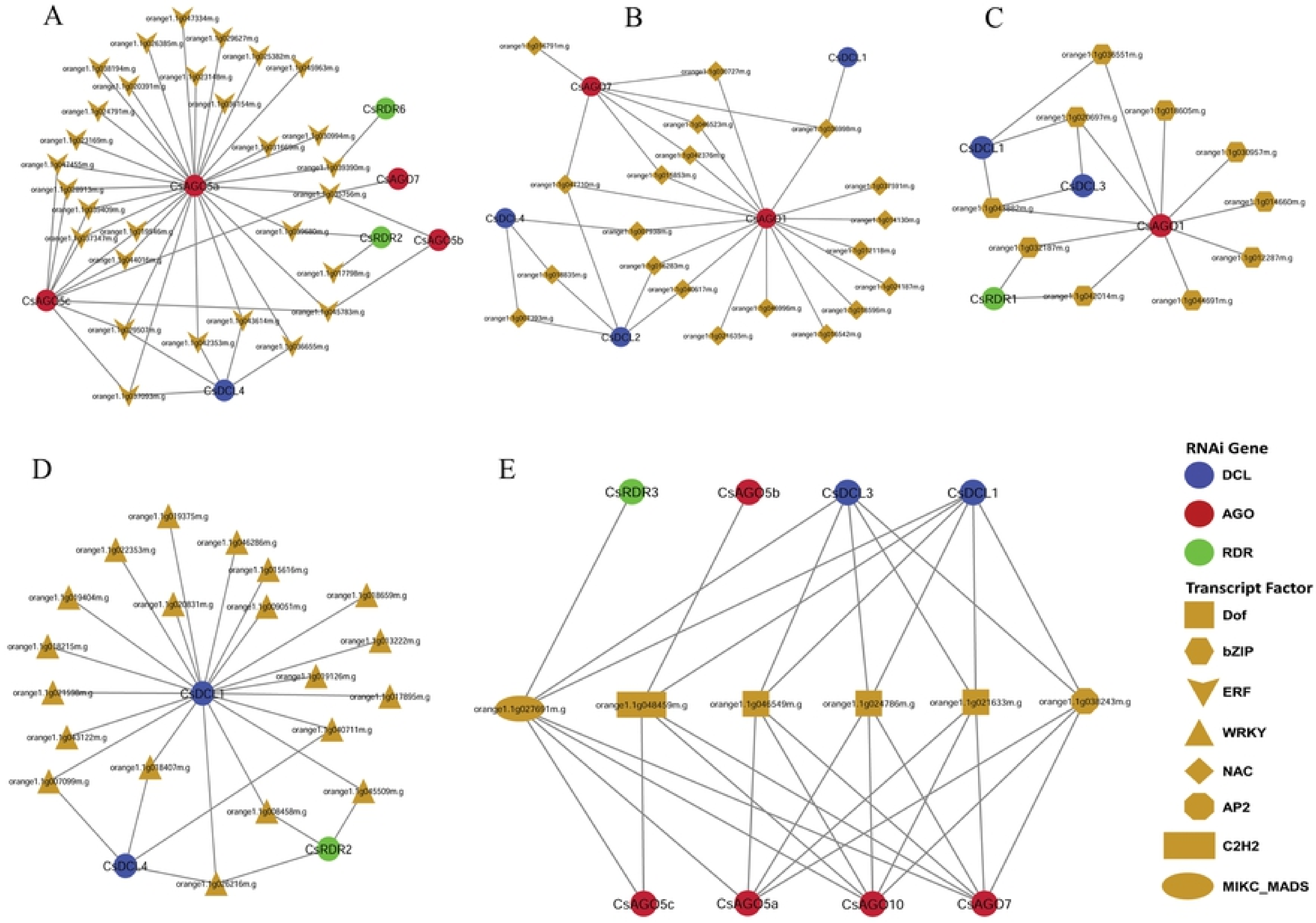
A
orange1.1g047334m.g
orange1.1g026385m.g
orange1.1g029627m.g
orange1.1g025382m.g
orange1.1g038194m.g
orange1.1g040963m.g
orange1.1g023148m.g
orange1.1g030391m.g
orange1.1g038734m.g
orange1.1g004791m.g
CsRDR6
orange1.1g030994m.g
orange1.1g023169m.g
orange1.1g031669m.g
orange1.1g047455m.g
orange1.1g039390m.g
CsAGO7
orange1.1g028913m.g
CsAGO5a
orange1.1g025756m.g
orange1.1g039409m.g
orange1.1g037347m.g
orange1.1g018946m.g
orange1.1g009680m.g
CsRDR2
CsAGO5b
orange1.1g044035m.g
orange1.1g017798m.g
CsAGO5c
orange1.1g045783m.g
orange1.1g043614m.g
orange1.1g025503m.g
orange1.1g042353m.g
orange1.1g036655m.g
orange1.1g037093m.g
CsDCL4
B
orange1.1g016791m.g
CsDCL1
orange1.1g008727m.g
CsAGO7
orange1.1g046523m.g
orange1.1g026098m.g
orange1.1g048376m.g
orange1.1g015853m.g
orange1.1g047210m.g
orange1.1g037101m.g
CsDCL4
CsAGO1
orange1.1g041130m.g
orange1.1g017938m.g
orange1.1g012118m.g
orange1.1g036283m.g
orange1.1g038835m.g
orange1.1g021187m.g
orange1.1g040617m.g
orange1.1g046096m.g
orange1.1g036096m.g
orange1.1g008283m.g
CsDCL2
orange1.1g024635m.g
orange1.1g036542m.g
C
orange1.1g038551m.g
orange1.1g018605m.g
orange1.1g020697m.g
CsDCL1
orange1.1g030957m.g
CsDCL3
orange1.1g014660m.g
orange1.1g043862m.g
CsAGO1
orange1.1g032187m.g
orange1.1g012287m.g
CsRDR1
orange1.1g042014m.g
orange1.1g044691m.g
D
orange1.1g019375m.g
orange1.1g046286m.g
orange1.1g022353m.g
orange1.1g015616m.g
orange1.1g019404m.g
orange1.1g020831m.g
orange1.1g020051m.g
orange1.1g018659m.g
orange1.1g018215m.g
orange1.1g013222m.g
orange1.1g039126m.g
orange1.1g021598m.g
CsDCL1
orange1.1g017895m.g
orange1.1g043122m.g
orange1.1g040711m.g
orange1.1g018407m.g
orange1.1g007099m.g
orange1.1g045509m.g
orange1.1g008458m.g
CsRDR2
CsDCL4
orange1.1g026216m.g
E
CsRDR3
CsAGO5b
CsDCL3
CsDCL1
orange1.1g027691m.g
orange1.1g048459m.g
orange1.1g046549m.g
orange1.1g024786m.g
orange1.1g021633m.g
orange1.1g038243m.g
CsAGO5c
CsAGO5a
CsAGO10
CsAGO7
RNAi Gene
DCL
AGO
RDR
Transcript Factor
Dof
bZIP
ERF
WRKY
NAC
AP2
C2H2
MIKC_MADS

Figure 10